New Ordered Metastable Phases between the Gel and Subgel Phases in Hydrated Phospholipids

Boris Tenchov,* Rumiana Koynova,* and Gert Rapp†
*Institute of Biophysics, Bulgarian Academy of Sciences, 1113 Sofia, Bulgaria, and †Max-Planck-Institute for Colloids and Interface Science, c/o HASYLAB, DESY, D-22603 Hamburg, Germany

ABSTRACT Formation of low-temperature ordered gel phases in several fully hydrated phosphatidylethanolamines (PEs) and phosphatidylcholines (PCs) with saturated chains as well as in dipalmitoylphosphatidylglycerol (DPPG) was observed by synchrotron x-ray diffraction, microcalorimetry, and densitometry. The diffraction patterns recorded during slow cooling show that the gel-phase chain reflection cooperatively splits into two reflections, signaling a transformation of the usual gel phase into a more ordered phase, with an orthorhombic chain packing (the Y-transition). This transition is associated with a small decrease (2–4 μl/g) or inflection of the partial specific volume. It is fully reversible with the temperature and displays in heating direction as a small (0.1–0.7 kcal/mol) endothermic event. We recorded a Y-transition in distearoyl PE, dipalmitoyl PE (DPPE), mono and dimethylated DPPE, distearoyl PC, dipalmitoyl PC, diC_{15}PC, and DPPG. No such transition exists in dimyristoyl PE and dilauroyl PE where the gel L_β phase transforms directly into subgel L_c phase, as well as in the unsaturated dielaidoyl PE. The PE and PC low-temperature phases denoted L_{R1} and SGII, respectively, have different hydrocarbon chain packing. The SGII phase is with tilted chains, arranged in an orthorhombic lattice of two-nearest-neighbor type. Except for the PCs, it was also registered in ionized DPPG. In the L_{R1} phase, the chains are perpendicular to the bilayer plane and arranged in an orthorhombic lattice of four-nearest-neighbor type. It was observed in PEs and in protonated DPPG. The L_{R1} and SGII phases are metastable phases, which may only be formed by cooling the respective gel L_β and $L_{\beta'}$ phases, and not by heating the subgel L_c phase. Whenever present, they appear to represent an indispensable intermediate step in the formation of the latter phase.

INTRODUCTION

Aqueous dispersions of polar lipids are known to form a large variety of phases depending on the chemical structure, temperature, and dispersing media. Their phase behavior is dominated by the main (order-disorder) phase transition associated with the melting of the lipid hydrocarbon chains. At temperatures above the main transition, lipids arrange in different liquid crystalline mesomorphic structures with lamellar and non-lamellar symmetry. Below the main transition, a basic equilibrium structure is the subgel (crystalline) L_c phase. In addition, a large number of intermediate stable, metastable, and transient lamellar gel structures are adopted by different lipids—with perpendicular or tilted chains with respect to the bilayer plane, with interdigitated, partially interdigitated, or non-interdigitated chains, rippled bilayers with various ripple periods, etc. Even so, the number of reported phases continues to grow. A prominent example in this respect is the recently documented by freeze-fracture subgel phase with concave-convex (egg carton) morphology in aqueous dispersions of DMPC and DPPC (Meyer et al., 2000). Thus, the lipid polymorphism at low temperatures still appears to be far from clear. Except as an approach to possible ways of cryodamage, its analysis is viewed as a source of quantitative knowledge concerning the process of domain formation and species demixing in the membranes.

The formation of a subgel phase usually requires a prolonged low-temperature equilibration. Taking advantage of its slow but still measurable kinetics, the gel-subgel transition in lipid multilayers has been the subject of numerous studies, mostly devoted to DPPC and other PCs (Ruocco and Shipley, 1982a, b; Nagle and Wilkinson, 1982; Ter-Minassian-Saraga and Madelmont, 1984; Akiyama, 1985; Akiyama et al., 1987; Kodama, 1986; Kodama et al., 1987; Slater and Huang, 1987; Tenchov et al., 1987, 1989; Tristram-Nagle et al., 1987, 1994; Yang and Nagle, 1988; Lewis and McElhaney, 1990, 1992; Pali et al., 1993; Koynova et al., 1995; Takahashi et al., 1996; Nagle et al., 1998), as well as to PEs (Harlos, 1978; Seddon et al., 1983; Lewis and McElhaney, 1993; Tenchov et al., 1999) and PGs (Wilkinson and McIntosh, 1986; Blaurock and McIntosh, 1986; Epand et al., 1992; Koynova, 1997). It has been shown by differential scanning calorimetry (DSC) that the appearance and growth of the "subtransition" in DPPC, concurrent with the growth of its equilibrium subgel L_c phase, is preceded by a small (~0.35 kcal/mol), readily reversible endothermic transition at ~7°C, manifesting fast, reversible formation of a metastable precursor of the L_c phase (Slater and Huang, 1987; Kodama et al., 1987). The metastable precursor phase, termed "sub-subgel" phase or SGII phase (Slater and Huang, 1987), differs from the gel $L_{\beta'}$ phase in its hydrocarbon chain arrangement (Koynova et al., 1995).

Similar low-temperature phase evolution exhibits dihexadecylphosphatidylethanolamine (DHPE) dispersed in water and in sucrose solutions (Tenchov et al., 1996, 1999). Upon cooling, the gel phase of DHPE undergoes a reversible, virtually non-hysteretic transition at 12°C where the hexag-

Received for publication 14 August 2000 and in final form 4 January 2001.
Address reprint requests to Dr. Boris Tenchov, Inst. Biophysics, Bulgarian Academy of Sciences, 1113 Sofia, Bulgaria. Tel.: (359-2)-971-3969; Fax: (359-2)-971-2493; E-mail: tenchov@obzor.bio21.bas.bg.

0006-3495/01/04/1873/18 $2.00

TABLE 1 Summary of the Y-transition calorimetric parameters

Lipid	Peak temperature T (°C)	Peak area* ΔH (kcal/mol)	Reference
DPPE	9.0	0.28	This work
DSPE	20.0	0.7	This work
DPPE-Me	9.2	0.48	This work
$DC_{15}PC$	5.2	0.17	This work
DPPC	7.5	0.35	This work
DPPC	6.8	0.25	Slater and Huang (1987)
DPPC	7.0	—	Kodama et al. (1987)
DPPC	8.1	0.35	Koynova et al. (1995)
DPPC, 100 mg/ml ethanol	6.0	—	Slater and Huang (1987)
DSPC	14.8	0.82	Koynova et al. (1995)
DSPC	10–20†	0.2	Snyder et al. (1996)
$DC_{20}PC$	15–35†	0.4	Snyder et al. (1996)
DPPG, 1 M NaCl, pH 7	11.7	0.33	This work
DHPE	12.5	0.22	Tenchov et al. (1999)
DHPE, 1 M NaCl, pH 7	~2	~0.46	Harlos and Eibl (1981)
DTPE, 1 M NaCl, pH 7	−2	0.07	Harlos and Eibl (1981)
DHPC	5.1	0.36	Laggner et al. (1987)
DTPA, 1 M NaCl, pH 4.6	1.5	0.08	Harlos and Eibl (1981)
DHPA, 1 M NaCl, pH 4.6	12	0.10	Harlos and Eibl (1981)

*The maximum peak area values recorded in the present work are given.
†It is supposed that a subgel phase might be involved in this transition (Snyder et al., 1996).

onal chain arrangement distorts into an orthorhombic one, while the lamellar period remains constant. These data disclosed a certain similarity between the low-temperature polymorphism of DHPE and that of the long-chain normal alkanes, known to form intermediate, metastable rotator (R) phases upon crystallization (Sirota et al., 1993; Sirota and Singer, 1994). To emphasize the parallelism with the alkane rotator phase R_I, we adopted the notation L_{R1}, referring to lamellar phase with untilted chains on orthorhombic lattice, for the low-temperature gel phase of DHPE. Here we report x-ray diffraction, calorimetric, and densitometric data demonstrating that similar transitions of the gel L_β or $L_{\beta'}$ phases into more ordered metastable low-temperature phases of L_{R1} or SGII type, respectively, also take place in a variety of other saturated phospholipids with intermediate chain length. The mechanism of the phase transformations in the different lipids looks similar to that observed in DPPC and DHPE. It is epitomized by reversible splitting of the wide-angle chain reflection, earlier termed the "Y-transition" (Tenchov et al., 1996, 1999). This splitting is accompanied by a small decrease or inflection of the specific volume of the lipid, while in heating direction the Y-transitions are invariably associated with small (0.1–0.7 kcal/mol) endothermic peaks. The L_{R1} and SGII phases formed in PEs and PCs, respectively, display two distinctly different kinds of hydrocarbon chain packing.

MATERIALS AND METHODS

Sample preparation

1,2-Dimyristoyl-*sn*-glycero-3-phosphoethanolamine (DMPE), 1,2-dipalmitoyl-*sn*-glycero-3-phosphoethanolamine (DPPE), 1,2-distearoyl-*sn*-glycero-3-phosphoethanolamine (DSPE), 1,2-dielaidoyl-*sn*-glycero-3-phosphoethanolamine (DEPE), 1,2-dipalmitoyl-*sn*-glycero-3-phosphoethanolamine-*N*-methyl (DPPE-Me), 1,2-dipalmitoyl-*sn*-glycero-3-phosphoethanolamine-*N*,*N*-dimethyl (DPPE-Me,Me), dimyristoyl-*sn*-glycero-3-phosphocholine (DMPC), 1,2-dipentadecanoyl-*sn*-glycero-3-phosphocholine ($DC_{15}PC$), 1,2-dipalmitoyl-*sn*-glycero-3-phosphocholine (DPPC), 1,2-distearoyl-*sn*-glycero-3-phosphocholine (DSPC), 1,2-dipalmitoyl-*sn*-glycero-3-[phospho-*rac*-(1-glycerol)](sodium salt) (DPPG) from Avanti Polar Lipids, Inc. (Birmingham, AL), and 1,2-dihexadecyl-*sn*-glycero-3-phosphoethanolamine (DHPE) from Fluka AG, Basel, Switzerland (>99% pure) were used without further purification. The lipids were found to migrate as a single spot in thin-layer chromatography checks. Microcalorimetric scans of their diluted dispersions showed highly cooperative chain-melting phase transitions at temperatures in agreement with the published values. Doubly distilled deionized water was added to weighed amounts of lipid. The dispersions were hydrated overnight at 20°C and cycled 8–10 times between ~10°C above the chain-melting transition and an ice bath. The samples were vortex-mixed at these temperatures for 1–2 min at each cycle. The lipid concentrations were 5–10 mg/ml for calorimetry, 20–30 mg/ml for densitometry, and 20–40 wt % for x-ray diffraction (XRD). For XRD measurements, samples were filled into glass capillaries (d = 1.0 mm) (Hilgenberg, Malsfeld, Germany) and flame-sealed. For some DSC and XRD measurements, "cold" samples were also used. These samples were homogenized by 5–10 successive cycles of freezing at −18°C, followed by thawing at temperature below 10°C and vortexing during the thawing step.

Differential scanning calorimetry

Microcalorimetric measurements were performed using high-sensitivity differential adiabatic scanning microcalorimeters DASM-1 M or DASM-4 (Biopribor, Pushchino, Russia) with sensitivity better than $4 \cdot 10^{-6}$ cal $\cdot$ K^{-1} and a noise level $<5 \cdot 10^{-7}$ W (Privalov et al., 1975). Heating runs, performed at a scan rate of 0.5°C/min, were followed by passive cooling in the calorimetric cell. Cooling from 20°C to 0°C together with the equilibration for the subsequent heating scan typically took ~1–1.5 h. The thermograms were corrected for the instrumental baseline. Transition en-

TABLE 2 Structural parameters of lipid gel and ordered gel phases

Lipid	WAX Spacings (nm) 110, −110	WAX Spacings (nm) 200	Distortion Parameter D	Lamellar repeat distance d (nm)	Reference
DPPE					This work
L_{R1} (−12°C)	0.419	0.388	0.100	6.02	
L_{R1} (0°C, 7 h)	0.418	0.396	0.071	6.03	
L_{β} (15°C)	0.413		0	6.15	
DSPE					This work
L_{R1} (−12°C)	0.418	0.381	0.120	6.52	
L_{β} (20°C)	0.412		0	6.62	
L_{β} (65°C)	0.424		0	6.43	
DSPE					Harlos (1978)
L_{R1}* (5°C)	0.418	0.388	0.097†	6.64	
gel (20°C)	0.411		0	6.64	
DEPE					This work
crystal (subgel)	—				
ordered gel	—				
gel (−10°C)	0.415		0	6.56	
gel (20°C)	0.424		0	6.51	
DPPE-Me,Me					This work
(0°C)‡	0.405	0.427	−0.072	6.07	
$L_{\beta'}$ (20°C)	0.418		0	6.07	
$L_{\beta'}$ (40°C)	0.420		0	6.08	
DMPC					This work
(−15°C)‡	0.399	0.434	−0.115	5.79	
$L_{\beta'}$ (10°C)	0.412	0.422	−0.032	5.92	
$DC_{15}PC$					This work
SGII (−15°C)	0.395	0.431	−0.120	5.97	
$L_{\beta'}$ (10°C)	0.408	0.421	−0.042	6.14	
DPPC					This work
SGII (−15°C)	0.392	0.428	−0.121	6.26	
$L_{\beta'}$ (20°C)	0.407	0.420	−0.042	6.38	
DPPC/1 M NaCl					This work
SGII (−5°C)	0.400	0.432	−0.109	6.15	
$L_{\beta'}$ (20°C)	0.414	0.423	−0.029	6.27	
DSPC					This work
SGII (−10°C)	0.397	0.433	−0.119	6.23	
$L_{\beta'}$ (25°C)	0.411	0.424	−0.042	6.35	
$DC_{24}PC$					Sun et al. (1996a, b)
L_{R1}* (25°C)	0.414	0.373	0.135†		
$L_{\beta'}$ (25°C)	0.394	0.438	−0.146		
L_{β} (75°C)	0.417		0		
DPPG/1 M NaCl pH 7.0					This work
SGII (−20°C)	0.401	0.431	−0.099	5.44	
$L_{\beta'}$ (25°C)	0.412	0.424	−0.039	5.87	
DPPG/1 M NaCl pH 1.0					This work
L_{R1} (−15°C)	0.418	0.378	0.130	6.71	
L_{β} (20°C)	0.411		0	6.71	
L_{β} (50°C)	0.420		0	6.62	
DHPE					Tenchov et al. (1999)
L_{R1} (−15°C)	0.420	0.379	0.133	6.21	
L_{β} (20°C)	0.414		0	6.21	
L_{β} (60°C)	0.427		0	6.08	
DHPC					Laggner et al. (1987)
$L_{i,O}$ (0–5°C)	0.420	0.380	0.129†	4.9	
gel (5–30°C)	0.410		0	4.8	
DHPA, pH 7					Jähnig et al. (1979)
L_{R1}* (5°C)	0.418	0.387	0.100†	5.96	
gel (20°C)	0.412		0	5.98	
DHPA, pH 12					Jähnig et al. (1979)
SGII* (5°C)	0.401	0.434	−0.108†	5.39	
gel (20°C)	0.410	0.428	−0.058†	5.46	
DTPE/1 M NaCl pH 7.0					Harlos and Eibl (1981)
L_{R1}* (−4°C)	0.413	0.394	0.062†	5.84	
gel (20°C)	0.413		0	5.82	
DTPA/1 M NaCl pH 4.6					Harlos and Eibl (1981)
L_{R1}* (−3°C)	0.414	0.387	0.088†	5.39	
gel (20°C)	0.411		0	5.39	

*Our assignment.

†Our calculation.

‡Unassigned ordered gel phase (see text for details).

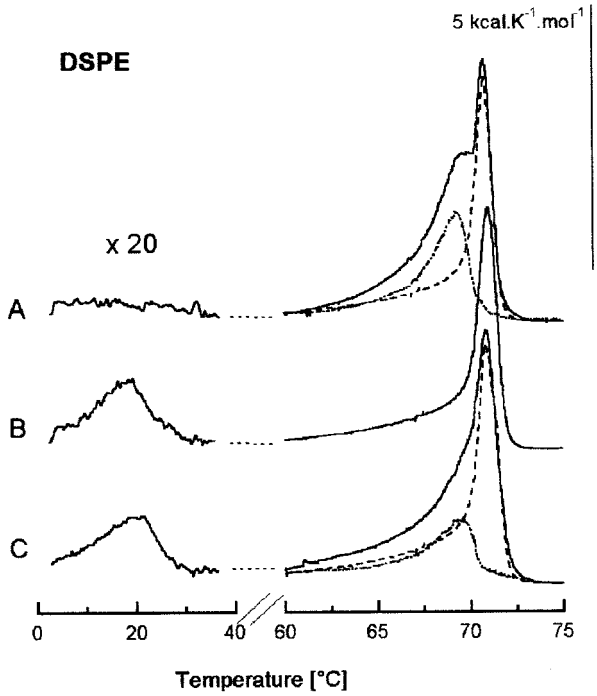

FIGURE 1 DSC heating thermograms of DSPE with different thermal prehistory. (*A*) First heating of a "cold" sample; (*B*) immediate reheating; (*C*) heating after storage for 30 min at −18°C, then for 7 days at 6°C. The vertical axis of the left panel is expanded 20 times with respect to the right panel. The L_β-L_α peak from thermogram *B* has been subtracted from *A* and *C* and the residuals ascribed to L_c-L_β transitions (*dashed lines*). Heating rate 0.5°C/min.

thalpies and temperatures were determined in a standard way, as previously described (Koynova et al., 1997a, b).

Synchrotron x-ray diffraction

For the synchrotron x-ray diffraction experiments a brass sample holder for glass capillaries was used. The holder was connected to a Peltier temperature control system as described recently (Rappolt and Rapp, 1996). This setup allows linear heating and cooling temperature scans at rates in the range 0.1–10°C/min. Diffraction patterns were recorded at beam lines X13, EMBL, and A2, HASYLAB, c/o DESY, Hamburg. The camera comprises a double focusing monochromator-mirror arrangement (Hendrix et al., 1979). X-ray reflections in the small- and wide-angle regimes were recorded simultaneously using a data-acquisition system previously described (Rapp et al., 1995). With this system, time-resolved experiments were feasible at high spatial resolution (Rapp et al., 1993). It consists of two linear detectors with delay line readout (Gabriel, 1977) connected electronically in series. In this configuration, both detectors appear as one single detector to the data-acquisition system (Boulin et al., 1988). One detector covers the small-angle region; the second detector covers the wide-angle region. To minimize the x-ray dose on the sample, a fast solenoid-driven shutter controlled by the data acquisition system was used to prevent irradiation of the sample in those periods when no diffraction data were taken. The signals of an ionization chamber to measure the incoming x-ray flux and the readings of a thermocouple placed in the sample holder next to the sample were stored together with the detector data. Some samples with longer exposure time were checked by thin layer chromatography after the experiments. However, no products of lipid degradation were detected in these samples and no radiation damage of the lipids was evident from their x-ray patterns. Linear heating-cooling scans were performed at rates 0.1–1°C/min. The data were processed using the interactive data-evaluating program OTOKO (Boulin et al., 1986). Wide-

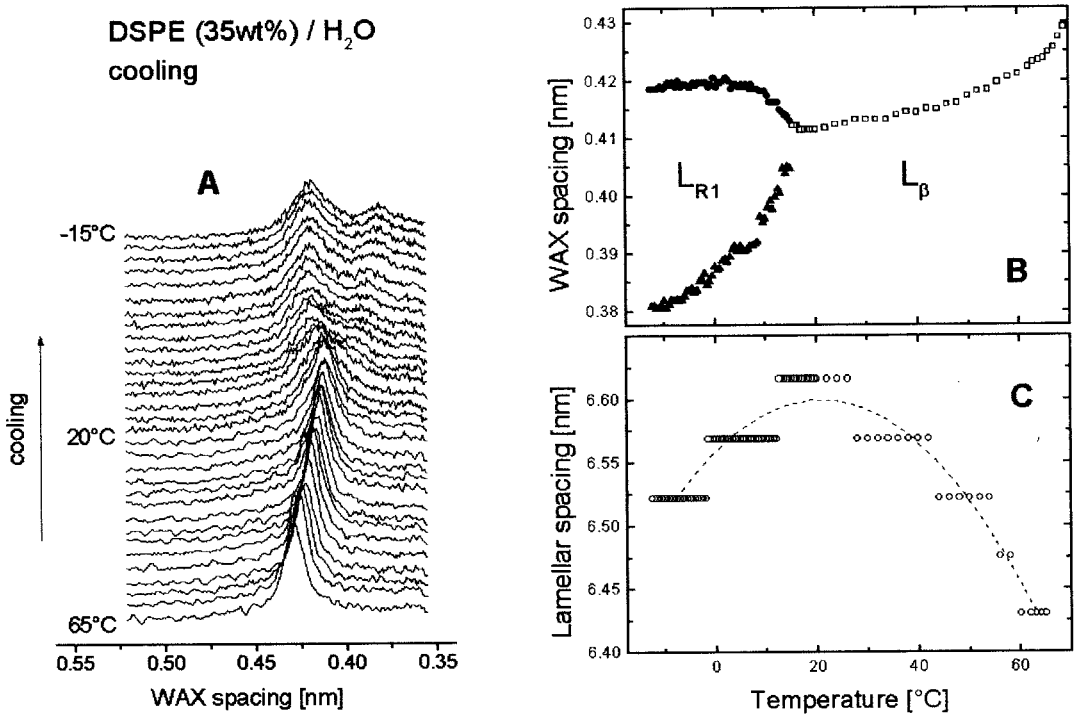

FIGURE 2 (*A*) Splitting of the WAX reflection of the DSPE gel phase upon cooling (2°C/min from 65° to 20°C, 0.1°C/min from 20° to −15°C); (*B*) WAX spacings; (*C*) lamellar repeat period.

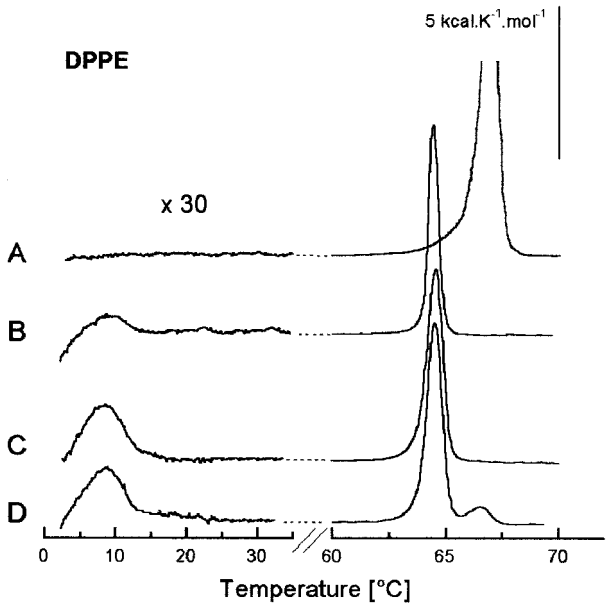

FIGURE 3 DSC heating thermograms of DPPE with different thermal prehistory. (*A*) First heating of a "cold" sample; (*B*) immediate reheating; (*C*) heating after storage for 2 h at 2–3°C; (*D*) heating after storage for 30 min at −18°C, then for 3 days at 0°C. The vertical axis of the left panel is expanded 30 times with respect to the right panel. Heating rate 0.5°C/min.

angle x-ray diffraction (WAX) patterns with overlapping peaks were analyzed by decomposition into Gaussian curves.

Differential scanning densitometry

The specific volume of the lipid molecules as a function of temperature was calculated from the density difference between water and the lipid dispersions. This difference was recorded with two DMA-602H cells (Anton Paar KG, Graz, Austria) connected to a home-built unit for data acquisition and temperature control. Linear heating and cooling scans of the samples were performed at 0.1–1°C/min with a PC-interfaced water bath. The instrument constants were determined according to the specifications of the producer, using distilled water and air as standards. The densities of air and water as a function of temperature were taken from the CRC Handbook of Chemistry and Physics (66th ed., 1985–1986). The partial specific volume $\bar{v}$ of lipids was calculated according to the equation $\bar{v} = 1/\rho_2(1 - (\rho_1 - \rho_2)/c)$, where ρ_1 and ρ_2 are the densities of the lipid dispersion and water, respectively, and c is the lipid concentration.

RESULTS

X-ray diffraction and calorimetric characterization of the Y-transition

In the present work we recorded a Y-transition in the following fully hydrated lipids: DSPE; DPPE; DPPE-Me;

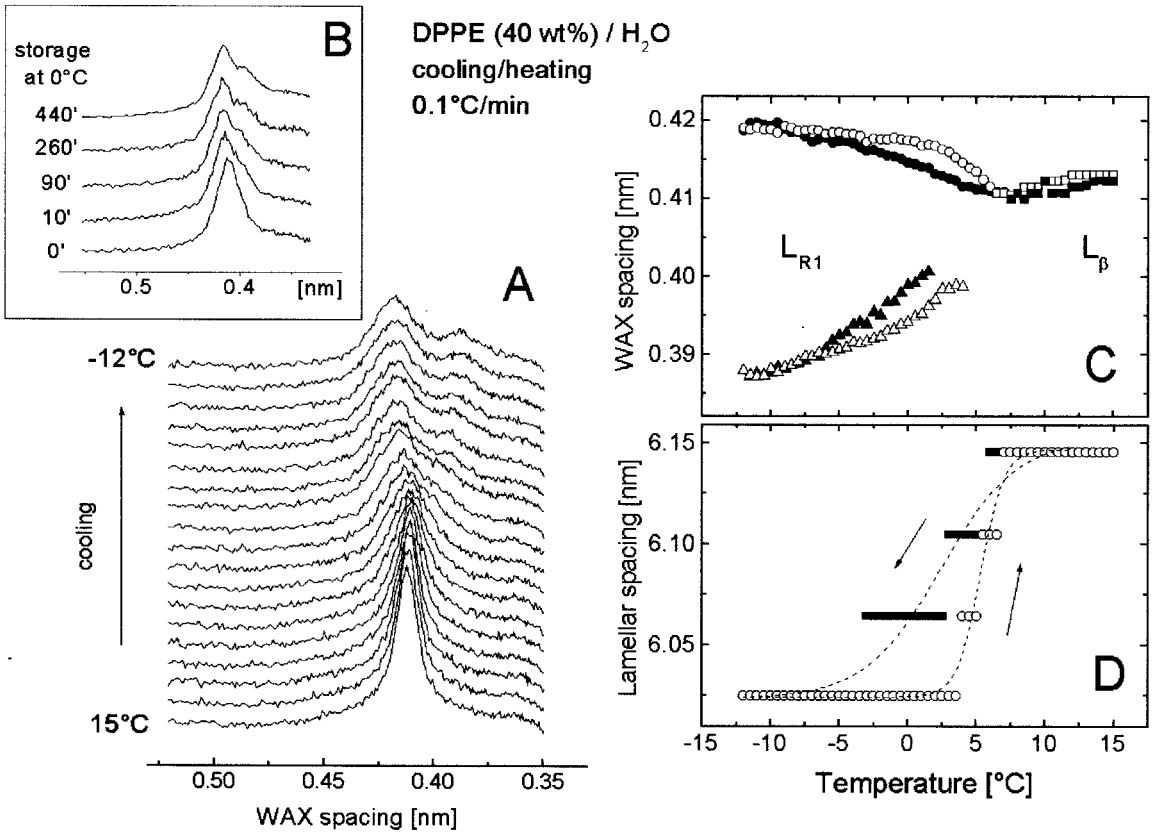

FIGURE 4 The Y-transition in DPPE. (*A*) WAX patterns recorded upon cooling at 0.1°C/min; (*B*) WAX patterns recorded at the indicated times of storage at 0°C after cooling at 0.5°C/min; (*C*) WAX spacings (cooling, solid symbols; heating, open symbols); (*D*) lamellar repeat period (cooling, solid symbols; heating, open symbols).

DPPE-Me,Me; DSPC, DPPC; $DC_{15}PC$; DPPG. No such transition was found to exist in DMPE and DLPE where the L_β phase transforms directly into subgel phase, as well as in the unsaturated DEPE, which appears to be unable to form more ordered gel or subgel phases. No conclusive evidence concerning the existence of a Y-transition in DMPC was obtained. Table 1 summarizes the thermodynamic parameters of the Y-transitions in the studied lipids; Table 2 summarizes the structural parameters of the gel, L_{R1}, and SGII phases. These tables also include surveys of previous work.

DSPE

Lipid dispersions, prepared by freeze-thawing ("cold" samples), undergo L_c-L_β and L_β-L_α transformations, which take place almost simultaneously, with ~1°C difference in the peak temperatures (Fig. 1*A*). In immediate second and further reheating, the L_β-L_α transition only remains at the higher temperature (70.8°C), and an additional peak (the Y-transition) is recorded at 20°C (Fig. 1 *B*). Two to three hours of incubation at 0–4°C slightly increase its area to a maximum value of 0.7 kcal/mol (Table 1). Low-temperature equilibrations for several days result in reappearance of the L_c-L_β transition at 69.6°C. The L_c phase recovery rate strongly depends on the equilibration protocol applied. At 20°C, the gel L_β phase is characterized by lamellar repeat spacing *d* of 6.62 nm and single, sharp chain reflection at 0.412 nm (Fig. 2; Table 2). Cooling to −15°C at 0.1°C/min results in decrease of *d* to 6.52 nm. At 17°C the chain reflection splits into two peaks denoting the onset of the Y-transition. Their positions progressively shift away and level off at 0.418 nm for the (110, −100) reflection and 0.381 nm for the (200) reflection at ~−10°C (Fig. 2 *B*). The L_{R1} phase formation proceeds in a similar way at cooling rates of 0.5–1°C.

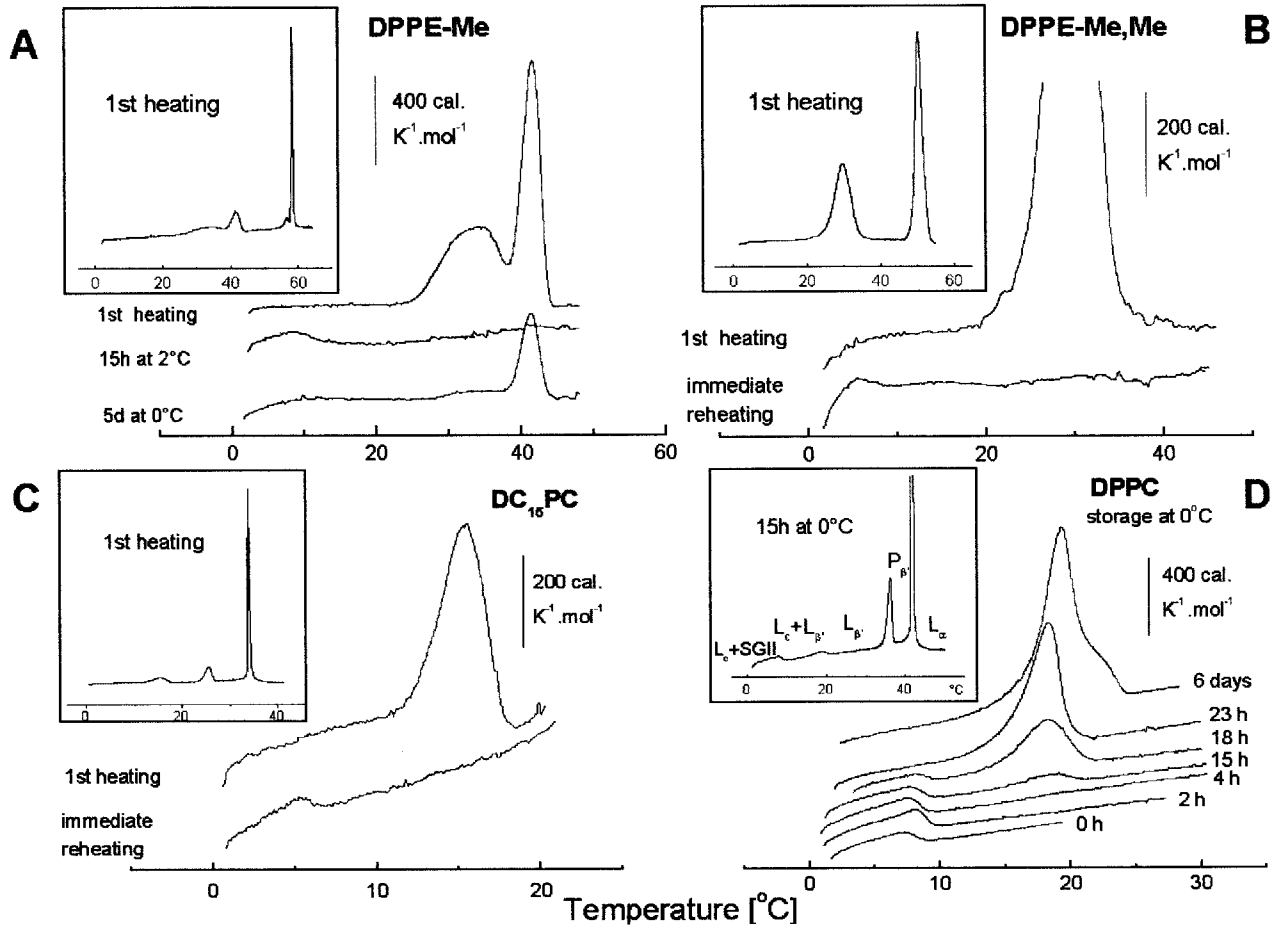

FIGURE 5 DSC heating thermograms (low-temperature portions). (*A*) DPPE-Me, with different thermal prehistory, as indicated; (*B*) DPPE-Me,Me: first heating after low-temperature sample preparation and immediate reheating after cooling to 0°C; (*C*) $DC_{15}PC$: first heating after low-temperature sample preparation and immediate reheating after cooling to 0°C; (*D*) DPPC recorded after the indicated incubations at 0°C (ice bath). The insets in (*A*)–(*C*) show full-scale thermograms of the initial heating of samples prepared at low temperature; the inset in (*D*) shows a full-scale thermogram of DPPC after 15 h storage at 0°C with all four transitions displayed. Heating rate 0.5°C/min.

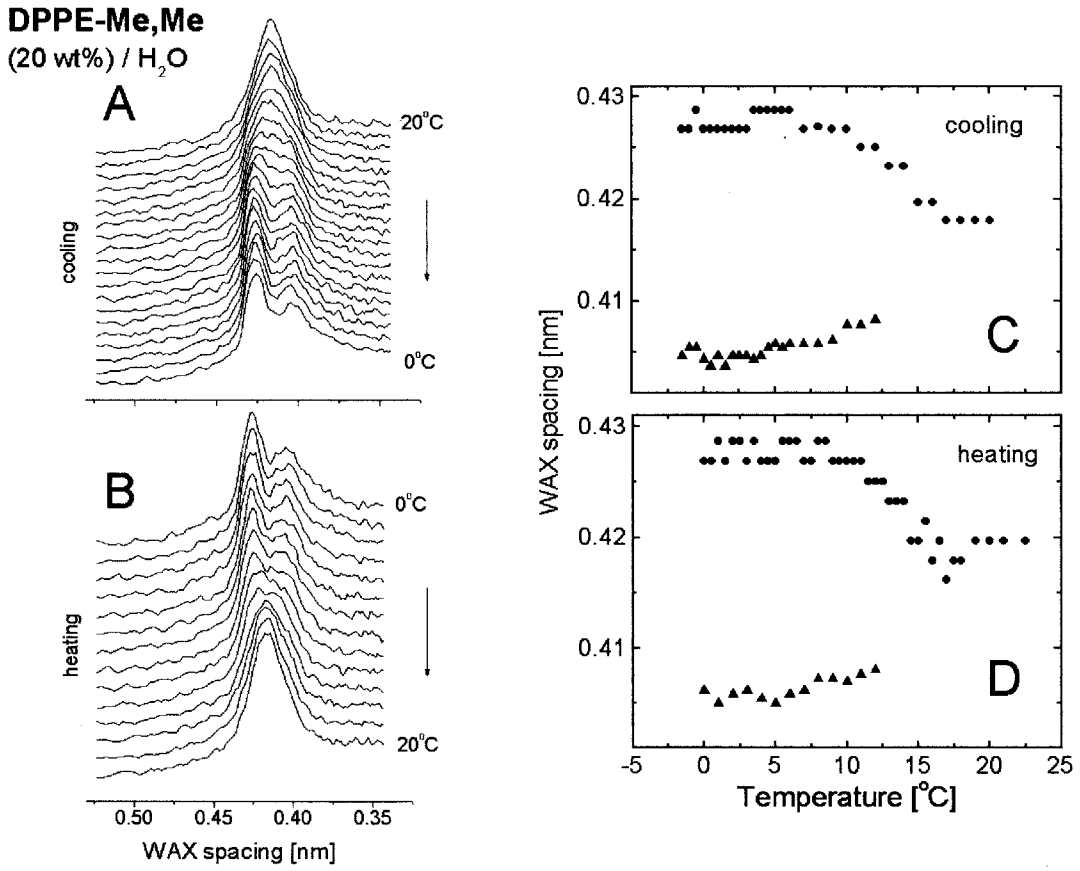

FIGURE 6 The Y-transition of DPPE-Me,Me during a cooling-heating cycle. (*A*) WAX patterns on cooling (1°C/min from 20° to 5°C and 0.5°C/min from 5° to 0°C); (*B*) WAX patterns on heating at 0.5°C/min; (*C*) WAX spacings on cooling. (*D*) WAX spacings on heating.

DPPE

With regard to the formation of an L_{R1} phase, the DPPE behavior is qualitatively similar to that of DSPE and differs mainly in a noticeably slower kinetics of the Y-transition.

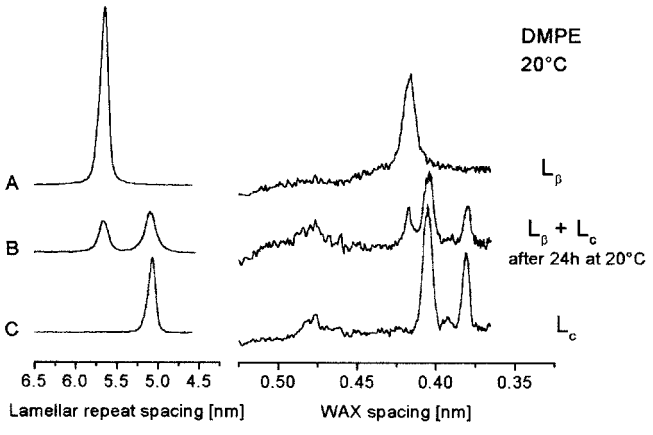

FIGURE 7 Direct conversion of the DMPE gel phase into subgel phase. (*A*) Immediately after cooling from the L_α phase; (*B*) after subsequent 24 h storage at 20°C; (*C*) the L_c phase of a "cold" sample.

"Cold" DPPE dispersions display a high-enthalpy L_c-L_α transition at 67°C upon first heating. In reheating scans, the L_c-L_α transition is replaced by an L_β-L_α transition at 64°C (Lipid Thermodynamic Database, LIPIDAT (http://www.lipidat.chemistry.ohio-state.edu); Koynova and Caffrey, 1994). Additionally, we observe a heat capacity peak (Y-transition) at ~9°C (Fig. 3). In immediate reheating the area of this peak is ~0.2 kcal/mol. It increases with some 50% upon 4–5 h of incubation at 0–4°C and reaches a value of ~0.3 kcal/mol (Table 1). The L_c-L_α transition at 67°C reappears after several day low-temperature equilibrations (Fig. 3). However, much longer (45 days) incubation of the sample at a temperature above the L_{R1}-L_β transition, at 20°C, does not even result in formation of traces of the L_c phase, as judged from the DSC thermograms.

At 15°C the lamellar gel L_β phase of DPPE is characterized by *d*-spacing of 6.15 nm and hexagonal chain arrangement with chain reflection at 0.413 nm. Cooling at 0.1°C/min results in splitting of the WAX reflection at 3–5°C and decrease of the *d*-spacing by some 0.1 nm (Fig. 4). The formation of the L_{R1} phase proceeds, however, on a perceptibly longer time scale in comparison to DSPE. Faster cooling to 0°C at 0.5–1°C/min only results in some widen-

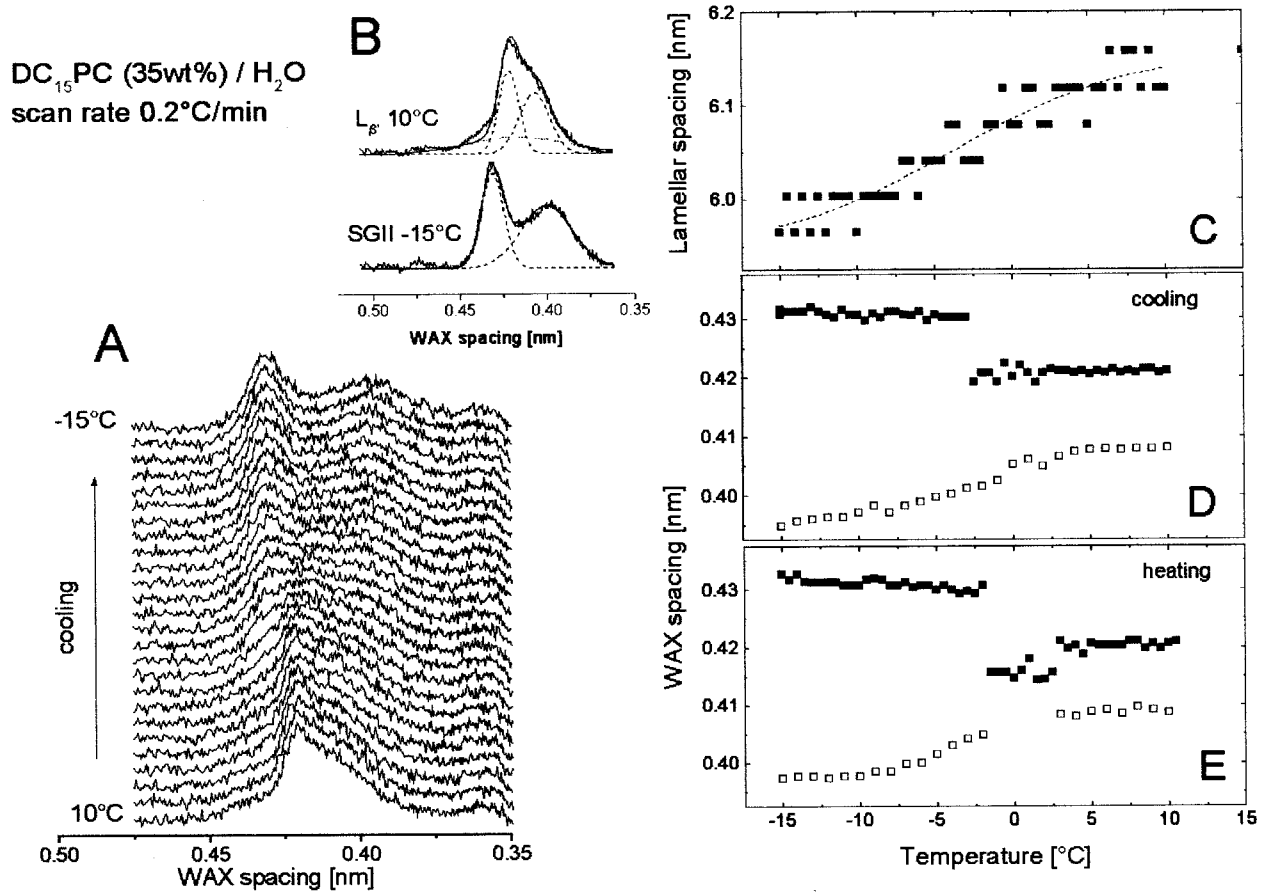

FIGURE 8 The Y-transition of $DC_{15}PC$ upon cooling-heating at 0.2°C/min. (*A*) WAX patterns recorded upon cooling; (*B*) WAX patterns at 10°C ($L_{\beta'}$ phase) and −15°C (SGII phase) decomposed into Gaussian curves; (*C*) lamellar repeat period upon cooling; (*D*) WAX spacings upon cooling; (*E*) WAX spacings upon subsequent heating.

ing of the WAX peak and minor decrease of *d* to 6.13 nm. Subsequent storage of the sample at 0°C produces advancing decrease of the lamellar repeat spacing down to 6.03 nm after 120 min. Equilibration for an additional 330 min at this temperature does not cause further decrease of *d* while, at the same time, the single chain reflection gradually splits into two peaks, placed at 0.396 and 0.418 nm after 445 min of low-temperature storage (Fig. 4 *B*). Heating of the sample reverts the split WAX reflection into a single, sharp WAX peak (Fig. 4 *C*) and restores the initial lamellar period of 6.15 nm (Fig. 4 *D*).

DPPE-Me

First heating of "cold" samples results in a double-peaked subtransition on the thermogram, with peak temperatures 34° and 41.6°C (Fig. 5 *A*). In immediate reheating, a small heat capacity anomaly (9°C, $\Delta H = 0.48$ kcal/mol; Table 1) is only observed below the chain-melting transition at 58.2°C. Upon low-temperature incubation, the subtransition at 41.6°C reemerges while the peak at 9°C decreases.

DPPE-Me,Me

A subtransition at 30°C is observed during the first heating of "cold" samples. There is however no clear evidence for its replacement by a low-temperature heat capacity anomaly in subsequent scans (Fig. 5 *B*). The subtransition at 30°C reappears after low-temperature equilibration. Aqueous dispersions of DPPE-Me,Me have been reported to form a gel phase with tilted chains at room temperature (Casal and Mantsch, 1983). It is characterized by *d*-spacing of 6.07 nm and chain reflection at 0.418 nm (Table 2). Cooling of the sample results in splitting of the wide-angle peak into two peaks that progressively disjoin in the range 15–10°C and level off at 0.405 nm and 0.427 nm at 0°C (Fig. 6). The Y-transition is fully reversible and proceeds with no change of the *d*-spacing.

DMPE and DLPE

No Y-transition exists in DMPE and DLPE. Cooling to −20°C produces no splitting of the DMPE gel phase WAX

reflection. The L_β phase of these lipids transforms directly, in a two-state process, into subgel L_c phase (see Fig. 7 for DMPE; Seddon et al. (1983) for DLPE).

DEPE

With aqueous DEPE dispersions we observed neither chain reflection splitting in the range from the chain-melting transition at 37°C to −12°C nor heat capacity anomalies in the range 0–37°C, indicating the absence of Y-transition in this lipid. Dispersion of DEPE in water forms lamellar gel L_β phase at 20°C, with $d = 6.51$ nm and single symmetric wide-angle reflection at 0.424 nm. Cooling to −12°C at 0.5–1°C/min produces a linear decrease of the WAX spacing to 0.415 nm without any change in its shape and width. A minor increase of the lamellar repeat period to 6.56 nm also takes place. These changes are reversible with the temperature (DEPE data not shown).

DMPC

In the cooling direction, DMPC undergoes L_α-$P_{\beta'}$-$L_{\beta'}$ phase sequence (LIPIDAT (see above); Koynova and Caffrey, 1998). At 10°C it is in the $L_{\beta'}$ phase, with lamellar repeat spacing of 5.92 nm. The wide-angle pattern displays a major reflection at 0.422 nm and a shoulder at 0.412 nm characteristic for tilted acyl chains. Upon further cooling at 0.1–1°C/min, these two peaks initially slightly move apart, then separate faster and reach values of ~0.40 nm and 0.43 nm at −15°C (Table 2). At the same time, the lamellar repeat period decreases to ~5.8 nm at −15°C. These changes are reversible on immediate reheating. Although suggestive for the existence of a Y-transition in the range below −5°C, the data are inconclusive, especially in the absence of supportive DSC and densitometric records. The characterization of this system was additionally obstructed by the water freezing at ~−15°C. The ice formation caused strong distortion of the diffraction patterns at temperatures below −15°C (DMPC data not shown).

$DC_{15}PC$

A small peak at 5°C is recorded in second heatings, instead of the subtransition at 15.6°C ($\Delta H = 1.5$ kcal/mol) observed upon first heating (Fig. 5 *C*, Table 1). The gel phase formed by this lipid at 10°C is characterized by lamellar repeat distance $d = 6.14$ nm and wide-angle pattern with major chain reflection at 0.421 nm and shoulder at 0.408 nm. Cooling at 0.2°C/min causes splitting of the chain reflection into two peaks, taking place at ~0°C. At −15°C the two reflections are at 0.395 nm and 0.431 nm, and the lamellar repeat distance has decreased to 5.97 nm (Fig. 8). This transformation is reversible on heating.

DPPC

Our present calorimetric observations of a small endotherm at 7°C in aqueous dispersions of DPPC (Fig. 5 *D*) are in full accord with previous reports (Slater and Huang, 1987; Kodama et al., 1987; see the Introduction). Following equilibration at 0°C, again in excellent agreement with those reports, the transition at 8°C ("sub-subtransition," as termed by Slater and Huang (1987); Y-transition in our notation) gradually disappears concomitantly with increase of the subtransition at 18°C, thus clearly manifesting a conversion of the SGII phase into L_c phase (Fig. 5 *D*). A full-scale thermogram with all four DPPC transitions displayed is shown in the inset of the figure. The Y-transition (an SGII-$L_{\beta'}$ transformation), as observed by XRD at scan rate of 0.2°C/min, is shown in Fig. 9. The structural data recorded in the present work agree with an earlier description of this transition (Koynova et al., 1995).

DSPC

The behavior of DSPC is similar to that of DPPC. It displays a small but well-reproducible calorimetric peak (Y-transition) at ~15°C (Koynova et al., 1995). The structural

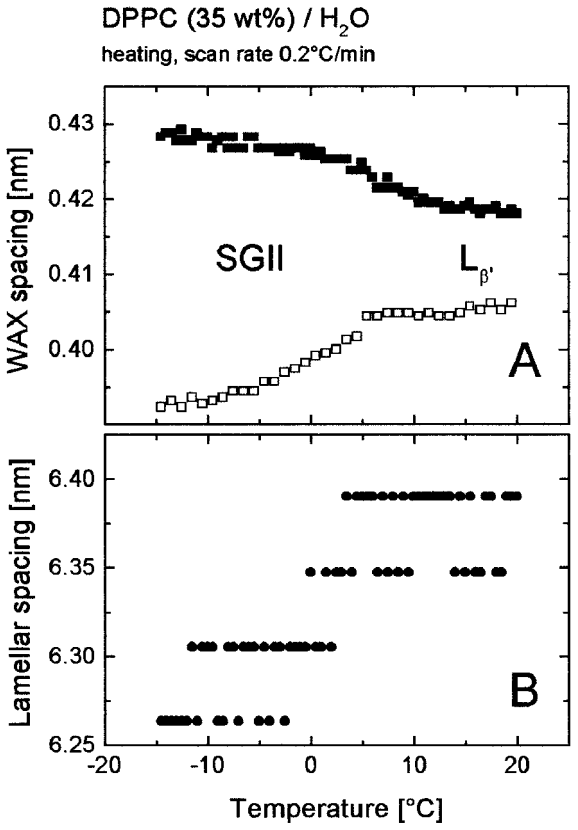

FIGURE 9 The DPPC Y-transition. Heating at 0.2°C/min, immediately after cooling from 20°C at 0.2°C/min: (*A*) WAX spacings; (*B*) lamellar repeat period.

changes during this transition recorded by XRD at scan rate of 0.1°C/min are shown in Fig. 10. These changes are reversible with the temperature.

DPPG

The titrable proton of DPPG has an apparent pK of 2.9 in 0.1 M salt (Watts et al., 1978). The DPPG dispersions studied here in 1 M NaCl solutions at pH 1.0 and pH 7.0 thus correspond to the protonated and the ionized state of the DPPG headgroup, respectively. Protonated DPPG is known to form gel phase with chains packed on hexagonal lattice and perpendicular to the bilayer plane, while ionized DPPG forms gel phase with tilted chains similar to that of the PCs (Watts et al., 1978, 1981).

Dispersion of DPPG in 1 M NaCl solution at pH 7.0 prepared at low temperature exhibits a high-enthalpy L_c-L_α transition (15.2 kcal/mol) at 43.6°C upon first heating, in accord with previous reports (Epand et al., 1992; Zhang et al., 1997). On immediate reheating after cooling to 0°C, a low-area peak (Y-transition) is recorded at 11.7°C on the thermogram, together with the pretransition $L_{\beta'}$-$P_{\beta'}$ at 40.5°C and the main $P_{\beta'}$-L_α peak at 42.4°C, as shown in Fig. 11. The cooling and heating scans in Fig. 12, *A* and *B* demonstrate that ionized DPPG undergoes a cooperative, reversible Y-transition centered at 12–13°C. At 25°C, the lamellar repeat spacing is 5.87 nm and the characteristic WAX pattern consists of a sharp major reflection at 0.424 nm (200) and a shoulder at 0.412 nm (110, −110). The Y-transition displays as precipitous separation of the (200) and (110, −110) peaks in the temperature range 14–11°C, to the values 0.401 and 0.431 nm at −20°C (Fig. 12 *C*). The lamellar spacing gradually decreases to 5.44 nm at −20°C (Fig. 12 *D*).

The behavior of DPPG dispersion in 1 M NaCl solution at pH 1.0 is illustrated in Fig. 13. At 50°C, it forms lamellar gel L_β phase, with lamellar repeat distance of 6.62 nm and sharp, symmetric WAX reflection at 0.420 nm. Cooling produces gradual shrinking of the hydrocarbon chain lattice, as visualized by the decrease of the WAX spacing to 0.411 nm at 20°C and 0.410 nm at 10°C. Splitting of the WAX peak into two reflections at ~8–6°C, signaling the Y-transition, interrupts this process. Lowering the temperature results in continuous further separation of the two wide-angle peaks to spacings of 0.378 nm and 0.418 nm at −15°C. This transformation is reversible on subsequent heating. The Y-transitions in ionized and protonated DPPG are well expressed also at a higher scan rate of 1°C/min.

Specific volume change at the Y-transition

The specific volume of the lipid experiences a small, reversible change at the Y-transition temperature (Fig. 14). The DPPE specific volume decreases by 3.5–4 μl/g at ~5°C upon cooling at 0.1°C/min (Fig. 14 *A*). During immediate reheating the reverse volume change takes place with a 7–8°C hysteresis, at about the temperature of the

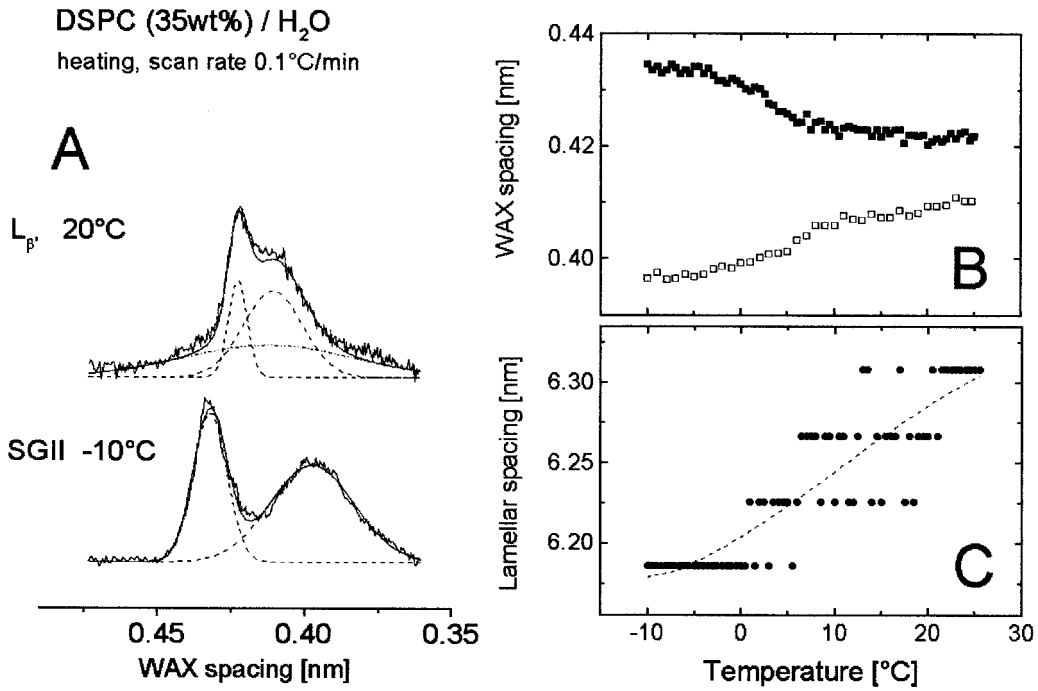

FIGURE 10 The DSPC Y-transition. Heating at 0.1°C/min, immediately after cooling from 25°C at 0.1°C/min. (*A*) WAX patterns of the $L_{\beta'}$ phase at 20°C and of the SGII phase at −10°C decomposed into Gaussian curves; (*B*) WAX spacings; (*C*) lamellar repeat period.

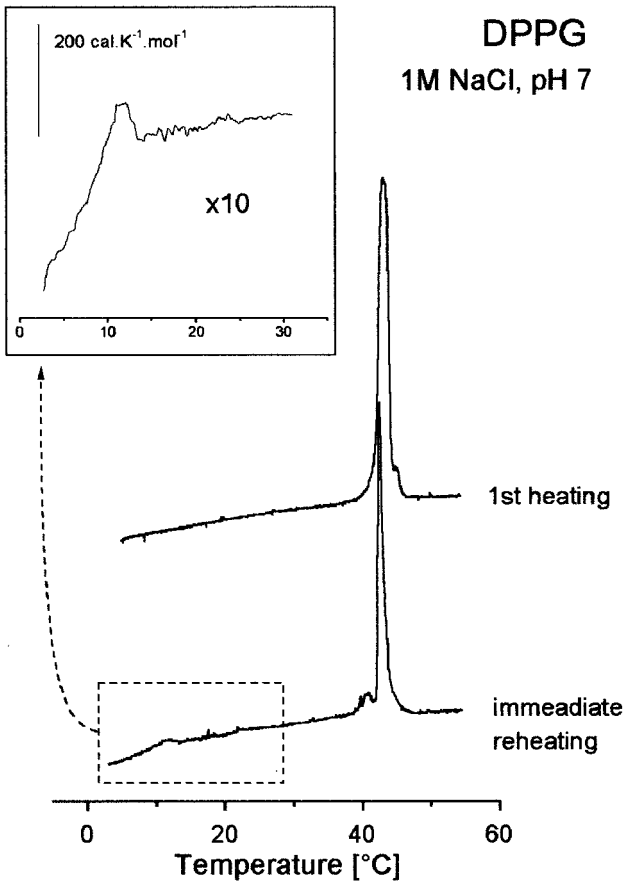

FIGURE 11 DSC heating thermograms of a DPPG dispersion in 1 M NaCl solution at pH 7. First heating after low-temperature sample preparation and immediate reheating after cooling to 0°C. Heating rate 0.5°C/min.

x-ray and calorimetric transitions. Noteworthy, no transition is observable at higher cooling rates of 0.5–1°C/min (data not shown). Instead, if the sample is cooled at a higher rate and then stored at 1–2°C in the densitometer, a slow isothermal decrease of the specific volume is recorded, in good accord with the slow transition kinetics recorded by x-ray diffraction. Another observation worth mentioning is the considerably improved reproducibility of the recorded densitograms if the gel DPPE phase has been equilibrated for several days at room temperature after cooling from the liquid-crystalline phase. As reported previously (Tenchov et al., 1999), the specific volume of DHPE decreases by 2 μl/g during the Y-transition (Fig. 14 *B*). This decrease is reversible upon reheating without prominent hysteresis and is reproducibly observable at scan rates in the range 0.1–0.5°C/min. The temperature dependence of the DPPC specific volume shows an inflection at ~7°C (Fig 14 *C*). This change is fully reversible and corresponds in temperature to the transitions recorded by DSC and x-ray diffraction.

DISCUSSION

Hydrocarbon chain packing in the L_{R1} and SGII phases

The gel phases of the PEs and PCs studied in the present work are known to exhibit two distinctly different kinds of hydrocarbon chain packing—hexagonal lattice with untitled chains exemplified by the L_β phase of DPPE (McIntosh, 1980) and "quasihexagonal" array with tilted chains in the $L_{\beta'}$ phase of the PCs (Tardieu et al., 1973). The gel L_β phases of DSPE and DPPE are characterized by sharp symmetric WAX reflections, indicative for untilted chains packed on hexagonal lattice. During the Y-transition ($L_\beta \rightarrow L_{R1}$), the WAX reflection splits into a strong band at ~0.42 nm and a weaker band at ~0.38 nm (Figs. 2 and 4). Such splitting indicates distortion of the hexagonal packing, with $d_{110} = d_{-110} = d_{200} \sim 0.41$ nm at 20°C, into orthorhombic packing with $d_{110} = {}_{d-110} \sim 0.42$ nm and $d_{200} \sim 0.38$ nm at −12°C. Identical evolution of the diffraction patterns takes place in DHPE dispersions as well, at virtually constant lamellar repeat period (Tenchov et al., 1999). Thus, the initial L_β hexagonal array transforms into the L_{R1} chain lattice by means of compression in next-to-nearest neighbor (NNN) direction. In this way four of the initial six nearest neighbors, located at the unit cell vertices, become closer to the central position than the remaining two. To distinguish this kind of chain packing from that in the PCs we refer to the PE chain lattice in the L_{R1} phase as orthorhombic lattice of four-nearest-neighbor type (Fig. 15 *B*). Such chain packing is typical for some long-chain alkanes in their metastable "rotator" R1 phase (see, e.g., Sirota et al., 1993).

The gel $L_{\beta'}$ phase of the PC series studied here is known to be tilted with respect to the bilayer normal. As evidenced by the shoulder at the high-angle side of the WAX reflection (Figs. 8, 10), the chain packing is "quasi-hexagonal," with two of the six nearest neighbors located slightly closer to the central position (Tardieu et al., 1973). Upon cooling, the WAX reflection disjoins further into d_{200} band and broad $d_{110} = d_{-110}$ band. This splitting is readily reversible upon immediate reheating. Its cooperativity was best expressed in $DC_{15}PC$ dispersions (Fig. 8) as well as in ionized DPPG (Fig. 12). Such evolution of the diffraction pattern shows that the initial "quasi-hexagonal" array of the $L_{\beta'}$ phase is compressed in nearest-neighbor (NN) direction, at 90° with respect to the direction of compression found for the PEs. Thus, the chain packing of the low-temperature SGII phase is orthorhombic, of two-nearest-neighbor type (see Fig. 15 *C* for an illustration). It is noteworthy that the decomposition of the WAX patterns shows that the additional very broad, low-height peak, required for best fit in the $L_{\beta'}$ phase and attributed to diffuse scattering (Sun et al., 1994), is not necessary for fitting the WAX pattern of the SGII phase (Figs. 8 *B* and 10 *A*).

The DPPG dispersions represent an interesting example of a lipid system, which can switch between the behavior of

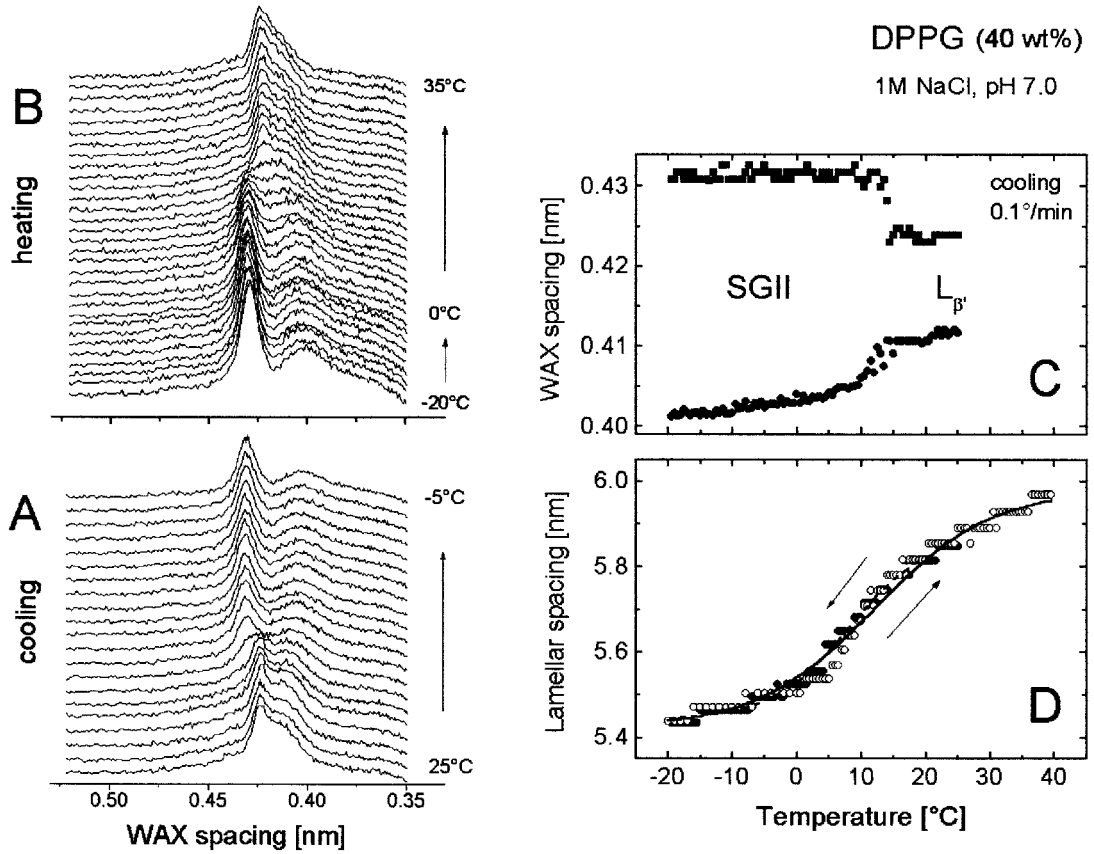

FIGURE 12 The Y-transition of DPPG dispersed in 1 M NaCl, pH 7.0. (*A*) WAX patterns recorded upon cooling at 0.1°C/min; (*B*) WAX patterns recorded on heating (−20–0°C at 0.2°C/min, 0–40°C at 0.1°C/min); (*C*) WAX spacings on cooling; (*D*) lamellar repeat period on cooling (*solid circles*) and heating (*open circles*).

the PEs and PCs, depending on the DPPG protonation status. In the protonated state DPPG forms gel L_β phase with chains perpendicular to the bilayer surface (Watts et al., 1978, 1981). Similarly to the PEs, upon cooling its L_β phase undergoes a clearly expressed and fully reproducible Y-transition into L_{R1} phase with orthorhombic chain packing of four-nearest-neighbor type (Fig. 13). Ionized DPPG bilayers in water display a tendency to unlimited swelling at neutral pH. In salt solutions, however, which screen the electrostatic repulsion, DPPG forms well-stacked lamellar phases and its phase behavior strongly resembles that of DPPC with sub, pre, and main transition. Below the pretransition (~35–40°C), DPPG forms a tilted $L_{\beta'}$ phase with hydrocarbon chain tilt of ~30° from the bilayer normal (Watts et al., 1981). Upon incubation at 2°C for several days, the DPPG molecules arrange in a subgel phase and a subtransition takes place at 15–30°C, depending on the electrolyte conditions (Wilkinson and McIntosh, 1986). The chain tilt in the subgel phase was estimated as 30–35° with respect to the bilayer normal (Blaurock and McIntosh, 1986). Here we demonstrate that, similarly to the PCs, the $L_{\beta'}$ phase of DPPG dispersed in 1 M NaCl solution at pH 7 undergoes a cooperative and fully reversible Y-transition, centered at 12–13°C, into an ordered gel phase of SGII type (Fig. 12).

The extent of distortion of the hexagonal (PEs; protonated DPPG) and "quasi-hexagonal" (PCs; ionized DPPG) chain packings during the Y-transition may be quantified by introducing a distortion order parameter. Such parameter can be generally defined as $D = 1 - (A/B)$, where A and B are the semiminor and semimajor axes of an ellipse drawn through the six nearest neighbors on the lattice (Sirota et al., 1993). Accordingly, $D = 0$ for hexagonally arranged chains and $D > 0$ in orthorhombic and oblique arrangements. To highlight the different kinds of chain packing in PEs and PCs, it is convenient to allow for D to also assume negative values. In the orthorhombic nomenclature this parameter converts to $D = 1 - (a/\sqrt{3}b)$, where a and b are the unit cell axes (Sirota et al., 1993). Using the last definition with $a = 2d_{200}$ and $b = 2d_{200}\tan(\arcsin(d_{110}/2d_{200}))$, we calculated the temperature dependence of D for the lipid systems studied (Fig. 16). The L_{R1} phases of the PEs and protonated DPPG are characterized by positive D values (Fig. 16, *top panel*), and the SGII phases of the PCs and ionized DPPG are characterized by negative D values (Fig. 16, *bottom panel*). While the sign of D highlights the kind of chain

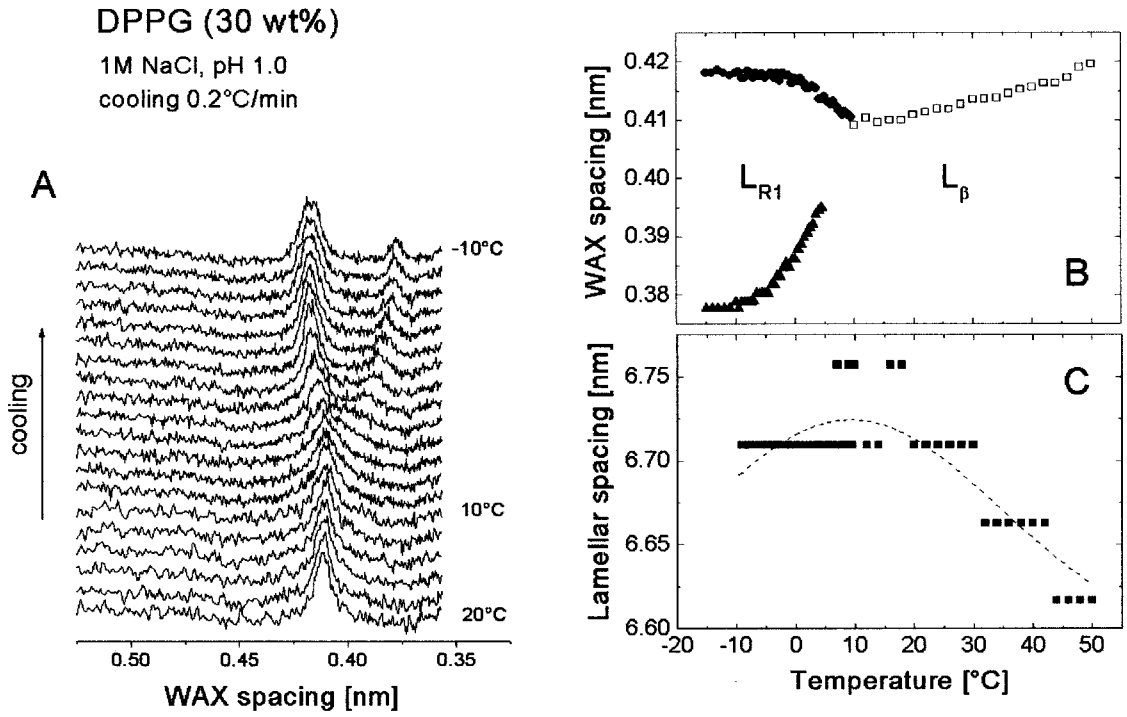

FIGURE 13 (*A*) Splitting of the WAX reflection of the gel phase of DPPG dispersed in 1 M NaCl, pH 1.0, upon cooling. Scan rates 1°C/min from 50° to 10°C and 0.2°C/min from 10° to −10°C; (*B*) WAX spacings; (*C*) lamellar repeat period.

packing (four-nearest- or two-nearest-neighbor type) in the phospholipid ordered gel phases, its temperature dependence gives a good measure for the cooperativity of the Y-transition.

Occurrence and properties of the Y-transition

In the present work, low-area (0.1–0.7 kcal/mol) transitions in the temperature range below 20°C were recorded by high-sensitivity DSC in fully hydrated lipids with different headgroups (PC; PE; PE-Me; PE-Me,Me; PG) and chain lengths (15, 16, 18 C-atoms). Similar low-temperature transitions were recorded calorimetrically also in aqueous dispersions of saturated dialkyl glucoglycerolipids (unpublished data). Albeit small, the observed excess heat capacity peaks are clearly and reproducibly observed in heating thermograms recorded immediately after cooling from high temperatures (Figs. 1, 3, 5, and 11). Short storage (1–2 h) at 0–2°C usually increases their cooperativity and area. The small but distinct change of the partial specific volume recorded by densitometry at the Y-transition well agrees in magnitude with the volume change calculated from the x-ray data (Tenchov et al., 1999). Both data sets show that the L_{R1} and SGII phases are slightly more compact than that extrapolated to the same temperature's respective L_β and $L_{\beta'}$ phases. The Y-transition is accompanied by no (e.g., DHPE) or small (≤2–3%) change of the lamellar repeat period *d*. An exception is the dispersion of charged DPPG at pH 7, which experiences a bigger reduction of *d* by some 0.4 nm (Fig. 12 *D*). Among a variety of factors that may contribute to the *d*-spacing changes is a minor change of the lipid hydration, i.e., that the Y-transition possibly takes place with modest water uptake on heating.

The data collected in the present work clearly indicate that the kinetics of the Y-transition depend on the chemical structure of the lipid. A salient example in this respect is represented by the DHPE/DPPE pair with alkyl and acyl chains, respectively. The Y- transition of DHPE is fast and proceeds with virtually no hysteresis at scan rates up to 1°C/min, while the respective transition in DPPE is much slower. It is only observable at very low cooling rates, or after several hours' equilibration at low temperature. We also noticed that the L_β-L_{R1} transformation kinetics in DPPE is sensitive to the time spent in the L_β phase. Samples that have been stored in the L_β phase for several days convert more easily to the L_{R1} phase as compared to samples just cooled from the liquid crystalline phase. This phenomenon possibly reflects a process of domain annealing in the L_β phase upon its storage at room temperature.

Mono and dimethylated DPPE (DPPE-Me and DPPE-Me,Me) also display a Y-transition (Fig. 5, *A* and *B*; Fig. 6) but it is not clear from the present data whether their low-temperature phase is of L_{R1} or SGII type. One may consider the result of Casal and Mantsch (1983) that these lipids form tilted gel phases as an indication that their low-temperature phases should be of SGII type (Table 2).

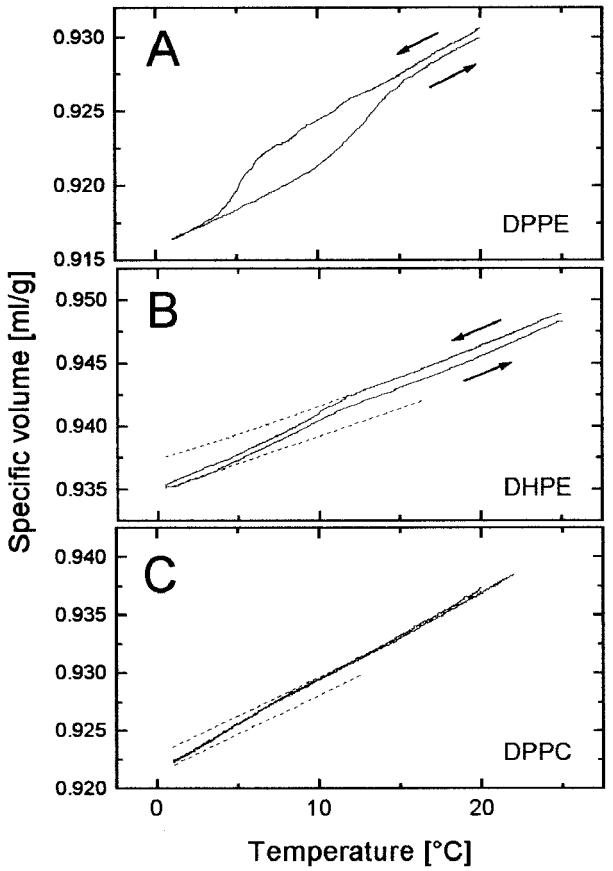

FIGURE 14 Lipid partial specific volumes. (*A*) DPPE, cooling-heating at rates of 0.1°C/min and 0.2°C/min, respectively. Before the measurement, the dispersion was stored for 5 days at room temperature after heating through the chain-melting transition. Lipid concentration 21 mg/ml; (*B*) DHPE, cooling-heating at 0.2°C/min. Lipid concentration 20 mg/ml; (*C*) DPPC, cooling-heating at 0.2°C/min. Lipid concentration 30 mg/ml.

The presence of solutes in the aqueous phase does not appear to obstruct the Y-transition. We found that the presence of up to molar concentrations of sucrose or trehalose does not interfere with the formation of the L_{R1} phase and has no influence on the properties of the Y-transition in DHPE dispersions (Tenchov et al., 1996). Likewise, DPPC dispersions in water and in 1 M NaCl solution display similar Y-transitions (unpublished data; Table 2). Another noteworthy observation is that the DPPC interdigitation induced by 100 mg/ml ethanol does not prevent the formation of the low-temperature gel phase (Slater and Huang, 1987). As noted by these authors, the low-temperature behavior of interdigitated DPPC resembles that of DHPC dispersed in excess water. The latter lipid is known to display a low-enthalpy transition at 5°C from an interdigitated gel phase with orthorhombic chain packing into interdigitated gel phase with hexagonal chain packing (Laggner et al., 1987; see Tables 1 and 2).

The structural changes during the Y-transitions typically coincide within a few degrees with the calorimetrically monitored thermal event. Because the formation of the ordered gel phases is sensitive to the sample thermal prehistory and to the scan rate, the differences between the transition temperatures, registered calorimetrically (e.g., the peak temperature) and by synchrotron XRD (e.g., the temperature of WAX splitting), could be a consequence of the different experimental protocols. A contribution from the different methods of temperature control in the DSC and XRD set-ups is also not excluded, as discussed before (Koynova et al., 1997b). Table 1 summarizes the peak temperatures of the Y-transitions determined by DSC.

A survey of the literature data shows that indications for ordered low-temperature gel phases with similar structural characteristics and fast formation kinetics have eventually been noticed also for other lipids. Harlos (1978) described a low-temperature phase transition in DSPE, referred to as "pretransition." It is characterized by transformation of the hydrocarbon chain packing from hexagonal into rectangular, reflected in splitting of the gel phase WAX reflection (Table 2). This transformation is rapid. It occurs without low-temperature incubation and does not bring about change in the lamellar repeat distance. It was, however, not detected calorimetrically. Nevertheless, there could be little doubt that the "pretransition" observed by Harlos (1978) corresponds to the DSPE Y-transition, characterized in the present work by DSC and synchrotron x-ray diffraction (Figs. 1 and 2; Tables 1 and 2). Phase transformations with similar characteristics were later reported also for ether-linked PAs and PEs with 14 and 16 carbon atoms in the hydrocarbon chains, in 1 M NaCl solutions ((Harlos and Eibl, 1981; Jähnig et al., 1979); see Tables 1 and 2).

The DSC data on the Y-transitions recorded in the present work are summarized in Table 1. This table also summarizes DSC data on transitions observed in previous work, which we consider to be Y-transitions as well. The Y-transition temperature increases with chain length with an increment of ~8–10°C per 2 CH_2 groups for both PEs (Fig. 17 *A*) and PCs (Fig. 17 *B*). The diagram in Fig. 17 *B* also includes data for long-chain PCs (chain lengths 20, 22, and 24 carbon atoms), as published by Snyder et al. (1996) and Sun et al. (1996a, b). A remarkable feature of their gel-to-ordered gel phase transition (G_d-G_o transition in the notation of Snyder et al. (1996)) is the change of the distortion sign upon this transformation. Although the G_d phase is tilted, of $L_{\beta'}$ type, no appreciable tilting takes place in the G_o phase (Sun et al., 1996a). In the notation adopted here, these longer-chain PCs therefore undergo an $L_{\beta'}$-L_{R1} transition.

Transitions similar to the lipid Y-transition take place in n-alkanes as well as in long-chain alcohols and similar molecules (Marconcelli et al., 1982; Ungar and Masic, 1985; Sirota et al., 1993; Sirota and Wu, 1996). These are transformations from a phase with hexagonally arranged

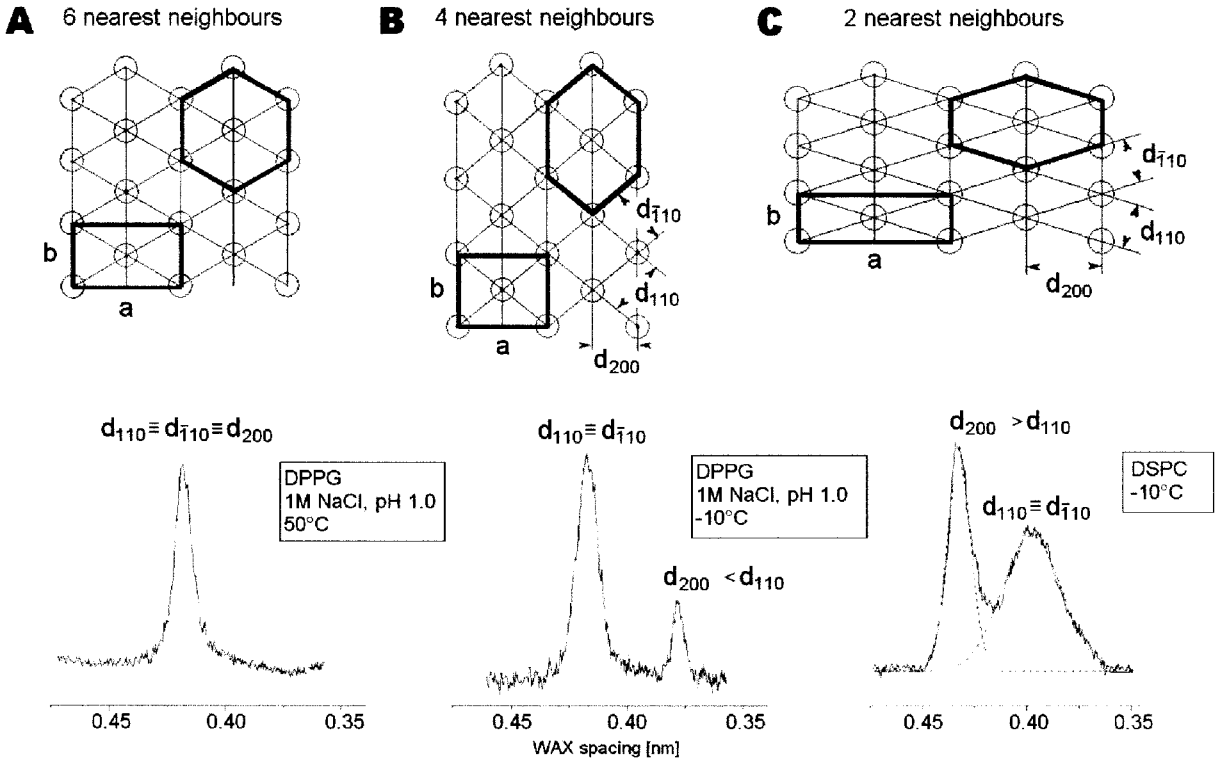

FIGURE 15 Hydrocarbon chain packing. (*A*) Hexagonal packing; (*B*) orthorhombic packing with four nearest neighbors; (*C*) orthorhombic packing with two nearest neighbors. Examples of WAX patterns corresponding to these packing motifs are shown.

hydrocarbon chains at higher temperatures to a phase, or to a sequence of phases, with orthorhombic chain arrangement at lower temperatures. All these phases are of "rotator" type, with a lack of long-range order with respect to the chain short-axis orientations and all molecular sites in the unit cell being crystallographically equivalent. Similarly to the L_β-L_{R1} transition in phospholipids, the hexagonal-to-orthorhombic phase transition in alkanes is characterized by very low latent heat (Ungar and Masic, 1985). To emphasize the parallelism with the alkane rotator phase R_I we adopted the notation L_{R1}, referring to a lipid lamellar gel phase with untilted chains on an orthorhombic lattice of four-nearest-neighbor type. This analogy indicates that the formation of the L_{R1} phase in the PEs and in DPPG at low pH should be considered as a consequence of the chains' packing properties rather than as due to headgroup and other interfacial interactions, which are absent in the alkane phases. For the lack of a direct analogy with the alkanes, we retained the notation SGII, introduced by Slater and Huang (1987) for the ordered phase observed at full hydration in the PCs and in ionized DPPG. It is conceivable that the structure of the SGII phase is influenced to a larger extent by the interactions at the lipid/water interface. It is pertinent to note in this connection that the PC headgroups occupy an area at the bilayer interface that is typically larger than the cross-section of the two hydrocarbon chains, by contrast with the PEs in which the headgroup is smaller than the chains' cross-section.

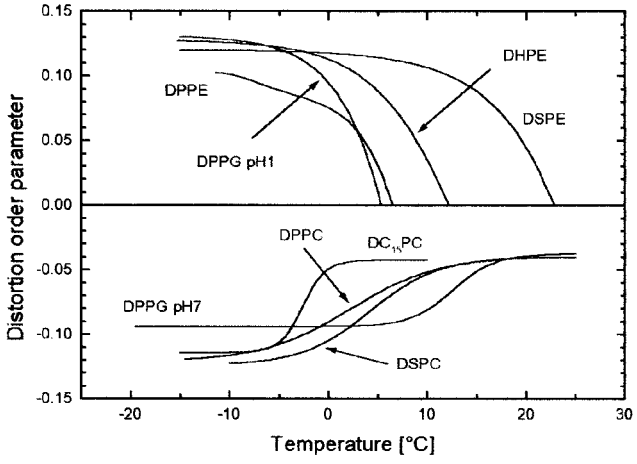

FIGURE 16 The distortion order parameter *D* during the Y-transition. Heating scan data recorded at 0.1°C/min, except for $DC_{15}PC$, DPPC, and protonated DPPG where the scan rate was 0.2°C/min.

Metastability of the ordered low-temperature gel phases

The L_{R1} and SGII gel phases of the lipid-water systems relax isothermally into the underlying subgel (crystalline)

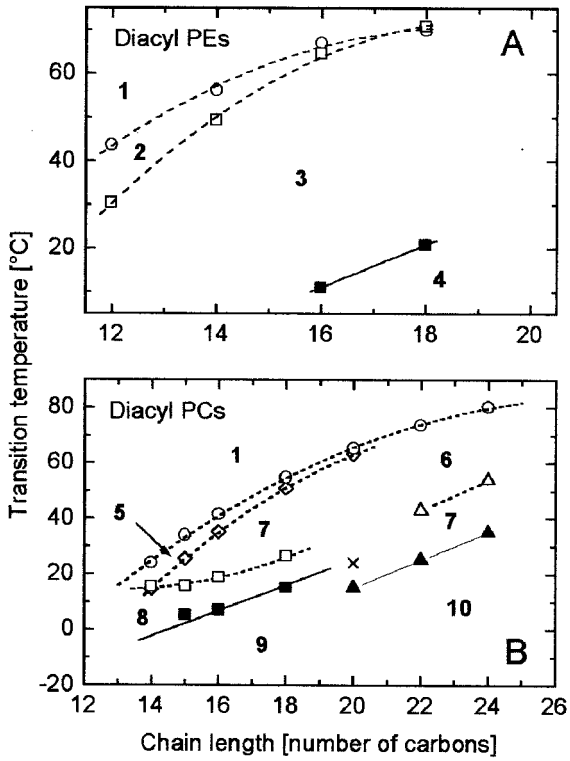

FIGURE 17 Transition temperatures as function of chain length for the PEs (*A*) and PCs (*B*) examined in the present work. The Y-transition line is the full line with solid squares; broken lines show the other transition lines. Transition temperatures of long-chain PCs ($DC_{20}PC$, $DC_{22}PC$, and $DC_{24}PC$) as registered by IR spectroscopy are also included; the cross indicates a transition recorded by calorimetry (Snyder et al., 1996). The numbers indicate phase regions as follows: 1) L_α; 2) L_c or metastable L_α; 3) L_c or metastable L_β; 4) L_c or metastable L_{R1}; 5) $P_{\beta'}$; 6) L_β; 7) $L_{\beta'}$; 8) $L_{c'}$ or metastable $L_{\beta'}$; 9) $L_{c'}$ or metastable SGII; 10) G_o (notation of Snyder et al., 1996), L_{R1} (our notation).

L_c phase upon low-temperature storage. The appearance of the L_c phase is evidenced by the emerging of initial traces of its transition endotherm into gel or liquid crystalline phase on the heating calorimetric thermograms (Figs. 1, 3, and 5). The gradual increase of this endotherm, concomitantly with decrease of the Y-transition peak, reflects the progressive conversion of the ordered gel phase into L_c phase (see, e.g., Fig. 5, *A* and *D*). The characteristic times for the formation of the L_c phase in the different lipid systems vary from hours to months and strongly depend on the equilibration protocol. In general, these times appear to be significantly shorter for the PCs in comparison to the PEs. In DPPC, for example, the first trace of the subtransition may be observed after several hours of incubation at 0–4°C. Once formed, an L_c phase does not revert into SGII or L_{R1} phase upon heating. Instead, it undergoes phase transformation at higher temperature into the usual gel phase (e.g., DPPC, DSPC, ionized DPPG, DHPE) or directly into the liquid crystalline state (e.g., DPPE, protonated DPPG). It is thus clear that the SGII and L_{R1} phases can only be entered by cooling of the usual gel phase. The phase sequences involving these phases are shown in Fig. 18. It should be pointed out that the Y-transitions studied here are always transitions between two metastable states—between an SGII or L_{R1} phase and a supercooled or entirely metastable L_β phase.

Whenever present, the ordered gel phases SGII and L_{R1} appear to be an obligatory prerequisite for the formation of an L_c phase, as illustrated in Fig. 18. The DPPC dispersion represents the best-documented example in this respect. When supercooled to the range below the subtransition but still above the Y-transition (8–14°C), the DPPC gel $L_{\beta'}$ phase does not convert into the subgel L_c phase even if stored for more than two months in this range (Yang and Nagle, 1988; Koynova et al., 1995). However, measurable quantities of the L_c phase start to appear within hours if the dispersion is kept at temperatures below the Y-transition in its SGII phase (Slater and Huang, 1987; Kodama et al., 1987). Several days of storage at 0–4°C are sufficient to complete the SGII-L_c transformation. A conversion (crystallization) of the supercooled $L_{\beta'}$ phase directly into the L_c phase may also be induced, but only by means of preceding storage of the sample for 7–10 h at a temperature below 7°C (Yang and Nagle, 1988; Tristram-Nagle et al., 1994). As demonstrated, such preliminary treatment is required to induce the appearance of stable portions (nuclei) of the L_c phase into the system which then serves to initiate a further growth of the L_c phase at a higher temperature in the range 8–14°C, from within the supercooled $L_{\beta'}$ phase. Since the delimiting temperature of 7°C, below which the L_c phase starts to form, is actually the temperature of the SGII-$L_{\beta'}$ phase transition, it is again evident that the initial formation of the subgel phase does take place only from within the SGII phase.

PEs with saturated chains of 15 and more C-atoms display similar behavior. Lewis and McElhaney (1993) did not observe L_c phase formation in such PEs after 3 years of storage at temperatures 1–5°C below the main transition, even after preceding 12 h incubation at −18°C. Our present observations on PEs of intermediate chain length invariably show that an L_c phase may only start to form at temperatures below the L_{R1}-L_β transition, and not upon incubation at temperatures above that transition. It is clear that the conversion of their metastable L_β phase directly into the crystalline L_c phase, although thermodynamically not forbidden, is kinetically hindered. Thus, the mechanism of L_c phase formation in a number of saturated PEs also appears to include an intermediate step to the L_{R1} phase, as already reported for DHPE (Tenchov et al., 1999).

The gel phase of the shorter-chain PEs (DMPE, DLPE; see Results) converts, however, directly into L_c phase, skipping the intermediate step to the L_{R1} phase, as shown in Fig. 18 *C*. Some short-chain PEs and PGs are also known to display liquid crystalline phase metastability in certain temperature ranges. It has been demonstrated that crystallization from the liquid crystalline phase is possible and really

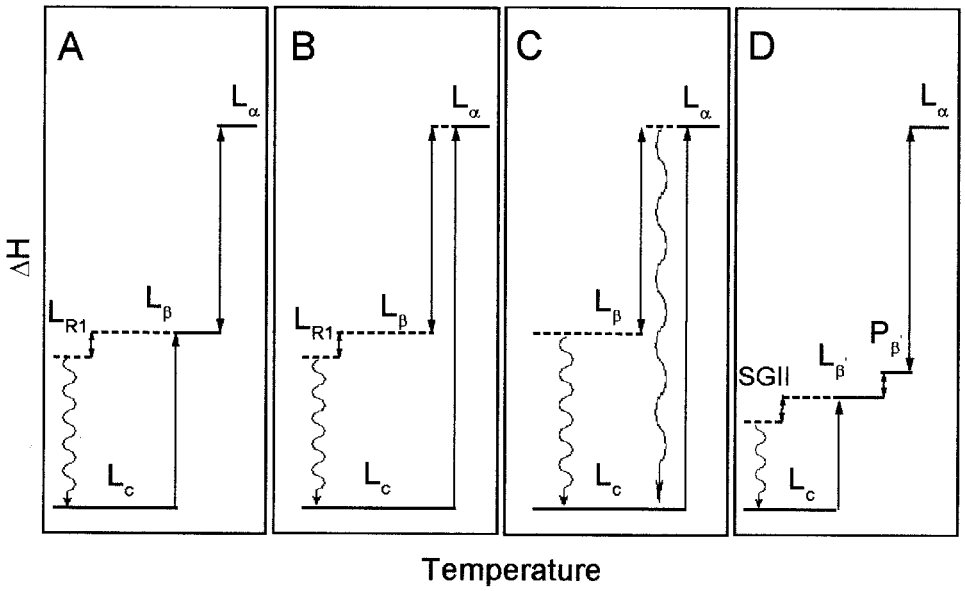

FIGURE 18 Transition pathways in fully hydrated lipids. Schemes *A* and *B* are representative for PEs of intermediate chain length and for protonated DPPG; scheme *C*, for short-chain PEs and PGs; *D*, for the PCs. Solid horizontal lines indicate stable phases; dashed lines, metastable phases. The wavy lines represent isothermal relaxation into the L_c phase. The metastable ripple phase of the PCs (Tenchov et al. (1989); Koynova et al. (1996)) is not shown in *D*, as it is irrelevant to the present study.

takes place in DLPE (Seddon et al., 1983), DMPG, and DLPG (Koynova, 1997). Thus, the L_α-to-L_c crystallization appears as another alternative to the pathways including an L_{R1} or SGII phase (Fig. 18 *C*).

In conclusion, a rapid, reversible transformation of the usual gel phase into a metastable, more ordered gel phase with orthorhombic hydrocarbon chain-packing at low temperatures turns out to be a common property for a large category of saturated phospholipids with intermediate chain length.

R.K. and B.T. acknowledge support from the Bulgarian Academy of Sciences and Deutsche Forschungsgemeinschaft.

REFERENCES

Akiyama, M. 1985. X-ray diffraction studies of subtransition in dipalmitoylphosphatidylcholine. *Jpn. J. Appl. Phys.* 24:231–234.

Akiyama, M., N. Matsushima, and Y. Terayama. 1987. Kinetics of the subtransition of multilamellar dipalmitoylphosphatidylcholine. *Jpn. J. Appl. Phys.* 26:1587–1591.

Blaurock, A. E., and T. J. McIntosh. 1986. Structure of the crystalline bilayer in the subgel phase of dipalmitoylphosphatidylglycerol. *Biochemistry.* 25:299–305.

Boulin, C., R. Kempf, A. Gabriel, and M. H. J. Koch. 1988. Data acquisition systems for linear and area x-ray detectors using delay line readout. *Nucl. Instrum. Methods.* 269:312–320*a*. (Abstr.).

Boulin, C., R. Kempf, M. H. J. Koch, and S. M. McLaughlin. 1986. Data appraisal, evaluation and display for synchrotron radiation experiments: Hardware and software. *Nucl. Instrum. Methods.* 249:399–407*a*. (Abstr.).

Casal, H. L., and H. H. Mantsch. 1983. The thermotropic phase behavior of N-methylated dipalmitoylphosphatidylethanolamines. *Biochim. Biophys. Acta.* 735:387–396.

CRC Handbook of Chemistry and Physics. 1985–1986. 66th Ed. R. C. Weast, editor. CRC Press, Boca Raton, FL.

Epand, R. M., B. Gabel, R. F. Epand, A. Sen, S. W. Hui, A. Muga, and W. K. Surewicz. 1992. Formation of a new stable phase of phosphatidylglycerols. *Biophys. J.* 63:327–332.

Gabriel, A. 1977. Position sensitive x-ray detector. *Rev. Sci. Instrum.* 48:1303–1305.

Harlos, K. 1978. Pretransitions in the hydrocarbon chains of phosphatidylethanolamines. *Biochim. Biophys. Acta.* 511:348–355.

Harlos, K., and H. Eibl. 1981. Hexagonal phases in phospholipids with saturated chains: phosphatidylethanolamines and phosphatidic acids. *Biochemistry.* 20:2888–2892.

Hendrix, J., M. H. J. Koch, and J. Bordas. 1979. A double focusing x-ray camera for use with synchrotron radiation. *Appl. Crystallogr.* 12: 467–472.

Jähnig, F., K. Harlos, H. Vogel, and H. Eibl. 1979. Electrostatic interactions at charged lipid membranes. Electrostatically induced tilt. *Biochemistry.* 18:1459–1468.

Kodama, M. 1986. Phase-transition phenomena induced by the successive appearances of new types of aggregation states of water-molecules in the L-DPPC water-system. *Thermochim. Acta.* 109:81–89.

Kodama, M., H. Hashigami, and S. Seki. 1987. Role of water molecules in the subtransition of the L-DPPC-water system as studied by differential scanning calorimetry. *J. Colloid Interface Sci.* 117:497–504.

Koynova, R. 1997. Liquid crystalline phase metastability in phosphatidylglycerols. *Chem. Phys. Lipids.* 89:67–73.

Koynova, R., J. Brankov, and B. Tenchov. 1997a. Modulation of the lipid phase behaviour by low-molecular solutes. *Eur. Biophys. J.* 25:261–275.

Koynova, R., and M. Caffrey. 1994. Phases and phase transitions of the hydrated phosphatidylethanolamines. *Chem. Phys. Lipids.* 69:1–34.

Koynova, R., and M. Caffrey. 1998. Phases and phase transitions of the phosphatidylcholines. *Biochim. Biophys. Acta.* 1376:91–145.

Koynova, R., A. Koumanov, and B. Tenchov. 1996. Metastable rippled gel phase in saturated PCs: calorimetric and densitometric characterization. *Biochim. Biophys. Acta.* 1285:101–108.

Koynova, R., B. Tenchov, and G. Rapp. 1997b. Mixing behavior of saturated short-chain phosphatidylcholines and fatty acids. Eutectic points, liquid and solid phase immiscibility, non-lamellar phases. *Chem. Phys. Lipids.* 88:45–61.

Koynova, R., B. G. Tenchov, S. Todinova, and P. J. Quinn. 1995. Rapid reversible formation of a metastable subgel phase in saturated diacylphosphatidylcholines. *Biophys. J.* 68:2370–2375.

Laggner, P., K. Lohner, G. Degovics, K. Muller, and A. Schuster. 1987. Structure and thermodynamics of the dihexadecylphosphatidylcholine-water system. *Chem. Phys. Lipids.* 44:31–60.

Lewis, R. N. A. H., and R. N. McElhaney. 1990. Subgel phases of n-saturated diacyl phosphatidylcholines: a Fourier-transform infrared spectroscopic study. *Biochemistry.* 29:7946–7953.

Lewis, R. N. A. H., and R. N. McElhaney. 1992. Structures of the subgel phases of n-saturated diacyl phosphatidylcholine bilayers: FTIR spectroscopic studies of $^{13}C = O$ and ^{2}H labeled lipids. *Biophys. J.* 61:63–77.

Lewis, R. N. A. H., and R. N. McElhaney. 1993. Calorimetric and spectroscopic studies of the polymorphic phase behavior of a homologous series of n-saturated 1,2-diacyl phosphatidylethanolamines. *Biophys. J.* 64:1081–1096.

Marconcelli, M., S. P. Qi, H. L. Strauss, and R. G. Snyder. 1982. Nonplanar conformers and the phase behavior of solid n-alkanes. *J. Am. Chem. Soc.* 104:6237–6247.

McIntosh, T. J. 1980. Differences in hydrocarbon chain tilt between hydrated phosphatidylethanolamine and phosphatidylcholine bilayers—molecular packing model. *Biophys. J.* 29:237–245.

Meyer, H. W., K. Semmler, W. Rettig, W. Pohle, A. S. Ulrich, S. Grage, C. Selle, and P. J. Quinn. 2000. Hydration of DMPC and DPPC at 4°C produces a novel subgel phase with convex-concave bilayer curvatures. *Chem. Phys. Lipids.* 105:149–166.

Nagle, J. F., S. Tristram-Nagle, H. Takahashi, and I. Hatta. 1998. Comment on Growth of Molecular Superlattice in Fully Hydrated Dipalmitoylphosphatidylcholine during Subgel Phase Formation Process. *Eur. Phys. J. B.* 1:399–400.

Nagle, J. F., and D. A. Wilkinson. 1982. Dilatometric studies of the subtransition in dipalmitoylphosphatidylcholine. *Biochemistry.* 21: 3817–3821.

Pali, T., R. Bartucci, L. I. Horvath, and D. Marsh. 1993. Kinetics and dynamics of annealing during sub-gel phase formation in phospholipid bilayers. *Biophys. J.* 64:1781–1788.

Privalov, P. L., V. V. Plotnikov, and V. V. Filimonov. 1975. Scanning microcalorimeters for studying macromolecules. *J. Chem. Thermodyn.* 7:41–47.

Rapp, G., A. Gabriel, M. Dosiere, and M. H. J. Koch. 1995. A dual detector single readout system for simultaneous small- (SAX) and wide-angle (WAX) scattering. *Nucl. Instrum. Meth. Phys. Res. A.* 357:178–182.

Rapp, G., M. Rappolt, and P. Laggner. 1993. Time-resolved simultaneous small- and wide-angle x-ray diffraction on DPPC by laser temperature-jump. *Prog. Coll. Polymer Sci.* 93:25–29.

Rappolt, M., and G. Rapp. 1996. Simultaneous small- and wide-angle x-ray diffraction during the main transition of dimyristoylphosphatidylethanolamine. *Ber. Bunsenges. Phys. Chem.* 100:1153–1162.

Ruocco, M. J., and G. G. Shipley. 1982a. Characterization of the subtransition of hydrated dipalmitoylphosphatidylcholine bilayers. X-ray diffraction study. *Biochim. Biophys. Acta.* 684:59–66.

Ruocco, M. J., and G. G. Shipley. 1982b. Characterization of the subtransition of hydrated dipalmitoylphosphatidylcholine bilayers. Kinetic, hydration and structural study. *Biochim. Biophys. Acta.* 691:309–320.

Seddon, J. M., K. Harlos, and D. Marsh. 1983. Metastability and polymorphism in the gel and fluid bilayer phases of DLPE. *J. Biol. Chem.* 258:3850–3854.

Sirota, E. B., H. E. King, D. M. Singer, and H. H. Shao. 1993. Rotator phases of the normal alkanes: an x-ray scattering study. *J. Chem. Phys.* 98:5809–5824.

Sirota, E. B., and D. M. Singer. 1994. Phase transitions among the rotator phases of the normal alkanes. *J. Chem. Phys.* 101:10873–10882.

Sirota, E. B., and X. Z. Wu. 1996. The rotator phases of neat and hydrated 1-alcohols. *J. Chem. Phys.* 105:7763–7773.

Slater, J. L., and C. Huang. 1987. Scanning calorimetry reveals a new phase transition in L-α-dipalmitoylphosphatidylcholine. *Biophys. J.* 52: 667–670.

Snyder, R. G., G. L. Liang, H. L. Strauss, and R. Mendelsohn. 1996. IR spectroscopic study of the structure and phase behavior of long-chain diacylphosphatidylcholines in the gel state. *Biophys. J.* 71:3186–3198.

Sun, W.-J., R. M. Suter, M. A. Knewtson, C. R. Worthington, S. Tristram-Nagle, R. Zhang, and J. F. Nagle. 1994. Order and disorder in fully hydrated unoriented bilayers of gel phase DPPC. *Phys. Rev. E.* 49: 4665–4676.

Sun, W.-J., S. Tristram-Nagle, R. M. Suter, and J. F. Nagle. 1996a. Anomalous phase behavior of long chain saturated lecithin bilayers. *Biochim. Biophys. Acta.* 1279:17–24.

Sun, W.-J., S. Tristram-Nagle, R. M. Suter, and J. F. Nagle. 1996b. Structure of gel phase saturated lecithin bilayers: temperature and chain length dependence. *Biophys. J.* 71:885–891.

Tardieu, A., V. Luzzati, and F. C. Reman. 1973. Structure and polymorphism of the hydrated chains of lipids: a study of lecithin-water phases. *J. Mol. Biol.* 75:711–733.

Takahashi, H., K. Hatta, and I. Hatta. 1996. Growth of molecular superlattice in fully hydrated DPPC during subgel phase formation process. *J. Phys. II France.* 6:1657–1662.

Tenchov, B., R. Koynova, M. Rappolt, and G. Rapp. 1999. An ordered metastable phase in hydrated phosphatidylethanolamine: the Y-transition. *Biochim. Biophys. Acta.* 1417:183–190.

Tenchov, B. G., L. J. Lis, and P. J. Quinn. 1987. Mechanism and kinetics of the subtransition in hydrated L-dipalmitoylphosphatidylcholine. *Biochim. Biophys. Acta.* 897:143–151.

Tenchov, B., M. Rappolt, R. Koynova, and G. Rapp. 1996. New phases induced by sucrose in saturated phosphatidylethanolamines: an expanded lamellar gel phase and a cubic phase. *Biochim. Biophys. Acta.* 1285:109–122.

Tenchov, B. G., H. Yao, and I. Hatta. 1989. Time-resolved x-ray diffraction and calorimetric studies at low scan rates. I. Fully hydrated dipalmitoylphosphatidylcholine (DPPC) and DPPC/water/ethanol phases. *Biophys. J.* 56:757–768.

Ter-Minassian-Saraga, L., and G. Madelmont. 1984. Subtransition and hydration studies of fully hydrated DPPC gel-phase. *J. Colloid Interface Sci.* 99:420–426.

Tristram-Nagle, S., R. M. Suter, W.-J. Sun, and J. F. Nagle. 1994. Kinetics of subgel formation in DPPC: x-ray diffraction proves nucleation-growth hypothesis. *Biochim. Biophys. Acta.* 1191:14–20.

Tristram-Nagle, S., M. C. Wiener, C.-P. Yang, and J. F. Nagle. 1987. Kinetics of the subtransition in dipalmitoylphosphatidylcholine. *Biochemistry.* 26:4288–4294.

Ungar, G., and N. Masic. 1985. Order in the rotator phase of n-alkanes. *J. Phys. Chem.* 89:1036–1042.

Watts, A., K. Harlos, and D. Marsh. 1981. Charge-induced tilt in ordered-phase phosphatidylglycerol bilayers. Evidence from x-ray diffraction. *Biochim. Biophys. Acta.* 645:91–96.

Watts, A., K. Harlos, W. Maschke, and D. Marsh. 1978. Control of the structure and fluidity of phosphatidylglycerol bilayers by pH titration. *Biochim. Biophys. Acta.* 510:63–74.

Wilkinson, D. A., and T. J. McIntosh. 1986. A subtransition in a phospholipid with a net charge, dipalmitoylphosphatidylglycerol. *Biochemistry.* 25:295–298.

Yang, C. P., and J. F. Nagle. 1988. Phase transformations in lipids follow classical kinetics with small fractional dimensionalities. *Phys. Rev. A.* 37:3993–4000.

Zhang, Y.-P., R. N. A. H. Lewis, and R. N. McElhaney. 1997. Calorimetric and spectroscopic studies of the thermotropic phase behavior of n-saturated 1,2-diacylphosphatidylglycerols. *Biophys. J.* 72:779–793.